Appendix A.39:

Palmers Rd – CPT 27040

Table 1: Site Description for Palmers Rd (CPT 27040).

Attribute	Yes/No			Description/Date	Symbol in Figure 1
	10-m Buffer	20-m Buffer	50-m Buffer		
Near a body of surface water or other free face features?	No	No	No	The center of the site is ~680 m to the NE from the Avon River (the free-face height is ~2m) and ~1180 m to the W from Pegasus Bay.	NA
Lateral spreading observed during the CES?	No	No	No	No lateral spreading was observed by the mapping team.[1]	NA
Nearby buildings or structures?	Yes	Yes	Yes	Building coverage of the 10-m, 20-m, and 50-m buffers is 21%, 26%, and 25%, respectively. The buildings are in the NW and SW quadrants of the 10-m buffer, the NW, SW, and SE quadrants of the 20-m buffers, and all quadrants of the 50-m buffer.	White Fill + Brown Outline
Sloping land?	No	No	No	Flat land, residential area	NA
Step changes in the ground surface?	No	No	No	NA	NA
Retaining walls?	No	No	No	NA	NA
Vegetation?	Yes	Yes	Yes	Trees and bushes cover 26, 17, and 18% of the 10-, 20-, and 50-m buffers, respectively. They are in all quadrants of all buffers.	White Fill + Green Outline
Anthropogenic changes to the site between the LiDAR surveys?	Yes	Yes	Yes	Building removal in the SE quadrant of the 50-m buffer between Mar 2013 and Aug 2013. Building removal and construction in the NW and SW quadrants of all buffers between Sep 2013 and Feb 2014. Building addition in all quadrants of all buffers between Feb 2014 and Aug 2014. Vegetation and building removal and building construction in the NW quadrant of the 50-m buffer between Aug 2014 and Jan 2015. Building removal in the N portion of the 50-m buffer between Jan 2015 and Apr 2015. Building addition at the same property in the N portion of the 50-m buffer between Apr 2015 and Jun 2015.	Building Addition/ Removal: Orange Crossline; Vegetation Removal: Green Crossline
Other important factors?	Yes	Yes	Yes	Low-motor-vehicle-volume, two-way roadway (Palmers Rd) occupies 2, 22, and 16% of the 10-, 20-, and 50-m buffers, respectively, and runs in the N-S direction through the NE and SE quadrants.	Road: Gray Fill + Red Outline

Note: Buffer is the area within a circle of a specified radius with CPT investigations done at its center (172.713519°, -43.498906°).

[1] Canterbury Geotechnical Database. (2012). "Observed Ground Crack Locations", Map Layer CGD0400 - 23 July 2012, retrieved July 09, 2018 from https://canterburygeotechnicaldatabase.projectorbit.com/

Figure 1: Site plan with areas where ejecta-induced settlement is considered.

Note 1: The patch (outlined in red) in the free field was selected for settlement assessment as an area free of vegetation and structures. Other important factors considered in the patch selection process were its proximity to a CPT, a property subjected to addition and/or demolition of a structure, front yard/backyard alterations (e.g., ploughing, rubble, scrap), and aerial distribution of sediment ejecta. In addition, the entire portion of the road within the 50-m buffer was considered for settlement assessment. Roads as hard, relatively flat surfaces provide many ground-classified points. Finally, the LiDAR-based settlement analyses were not conducted for the Sep-10 EQ due to the evident absence of ejecta from Patch A and Road. The Oct 2015 LiDAR survey was not considered for the settlement analysis of Patch A due to the anthropogenic changes.

Table 2: LiDAR flight error adjustments, global adjustments for the difference between average LiDAR point elevations and benchmark survey elevations, and vertical tectonic movement adjustments.

	Adjustments (mm)		
Earthquake Event(s)	LiDAR Flight Error	Global Offset[2]	Tectonic Vertical Movement
Sep-10	-100	-3	0
Feb-11	0	16	-30
Jun-11	0	38	-40
Dec-11	0	-65	0
CES	-100	-14	-70
Any LiDAR survey affected by ejecta?			No

Note: The negative sign indicates the subtraction from the ground surface subsidence, while the positive sign indicates the addition to the ground surface subsidence.

Table 3a: LiDAR Measurement Error for Patch A.

Surveys	Buffer	Area Averaged Difference Indicating Repeat Measurement Error (mm)	$\sigma^*_{\text{individual LiDAR points}}$ (mm)	%Reduction in σ due to Area Averaging of LiDAR Points
Post Feb 2011: Mar 2011 and May 2011	10-m	59	59	[100,100]
	20-m	59		
	50-m	59		
Post Dec 2011: Feb 2012 and Oct 2015	10-m	ND	70	[ND,ND]
	20-m	ND		
	50-m	ND		

*Standard deviation; ND = Not determined.

[2] Russell, J., & van Ballegooy, S. (2015). *Canterbury Earthquake Sequence: Increased liquefaction vulnerability assessment methodology*. New Zealand: Tonkin & Taylor Ltd.

Table 3b: LiDAR Measurement Error for Road.

Surveys	Buffer	Area Averaged Difference Indicating Repeat Measurement Error (mm)	σ*$_{\text{individual LiDAR points}}$ (mm)	%Reduction in σ due to Area Averaging of LiDAR Points
Post Feb 2011: Mar 2011 and May 2011	10-m	NA	59	[47,47]
	20-m	ND		
	50-m	28		
Post Dec 2011: Feb 2012 and Oct 2015	10-m	NA	70	[59,59]
	20-m	ND		
	50-m	41		

*Standard deviation; ND = Not determined; NA = Not available.

Table 4a: Ground surface subsidence adjustments due to LiDAR measurement error for Patch A.

Earthquake Event(s)	$\sigma_{\text{pre-EQ LiDAR survey}}$ (mm)	$\sigma_{\text{post-EQ LiDAR survey}}$ (mm)	σ_{total} (mm)	Area Average Adjusted σ (mm) **
Sep-10	158	56	134	±134
Feb-11	56	59	59	±59
Jun-11	59	61	62	±62
Dec-11	61	70	87	±87
CES	158	70	124	±124

**Based on the highest %Reduction in Table 3a.

Table 4b: Ground surface subsidence adjustments due to LiDAR measurement error for Road.

Earthquake Event(s)	$\sigma_{\text{pre-EQ LiDAR survey}}$ (mm)	$\sigma_{\text{post-EQ LiDAR survey}}$ (mm)	σ_{total} (mm)	Area Average Adjusted σ (mm) **
Sep-10	158	56	134	±79
Feb-11	56	59	59	±35
Jun-11	59	61	62	±36
Dec-11	61	70	87	±51
CES	158	70	124	±73

**Based on the highest %Reduction in Table 3b.

Table 5a: Raw liquefaction-related ground surface subsidence using original LiDAR points for Patch A.

	Average Ground Surface Subsidence (mm)		
Earthquake Event(s)	10-m Buffer	20-m Buffer	50-m Buffer
Sep-10	ND	ND	ND
Feb-11	-118	-118	-118
Jun-11	95	95	95
Dec-11	84	84	84
CES	ND	ND	ND

Table 5b: Raw liquefaction-related ground surface subsidence using original LiDAR points for Road.

	Average Ground Surface Subsidence (mm)		
Earthquake Event(s)	10-m Buffer	20-m Buffer	50-m Buffer
Sep-10	NA	ND	ND
Feb-11	NA	ND	76
Jun-11	NA	ND	80
Dec-11	NA	ND	45
CES	NA	ND	ND

Table 6a: Corrected liquefaction-related ground surface subsidence using original LiDAR points for Patch A with the calculated adjustments in Table 2.

	Average Calculated Ground Surface Subsidence (mm)		
Earthquake Event(s)	10-m Buffer	20-m Buffer	50-m Buffer
Sep-10	ND	ND	ND
Feb-11	-132±50	-132±50	-132±50
Jun-11	93±50	93±50	93±50
Dec-11	19±75	19±75	19±75
CES	ND	ND	ND

Notes: Plus/minus values are same as those in Table 4a, but rounded to the nearest 25 mm; Positive overall values indicate ground surface subsidence, while negative overall values indicate ground surface uplift; ND = Not determined.

Table 6b: Corrected liquefaction-related ground surface subsidence using original LiDAR points for Road with the calculated adjustments in Table 2.

Earthquake Event(s)	Average Calculated Ground Surface Subsidence (mm)		
	10-m Buffer	20-m Buffer	50-m Buffer
Sep-10	NA	ND	ND
Feb-11	NA	ND	62±25
Jun-11	NA	ND	78±25
Dec-11	NA	ND	-20±50
CES	NA	ND	ND

Notes: Plus/minus values are same as those in Table 4b, but rounded to the nearest 25 mm; Positive overall values indicate ground surface subsidence, while negative overall values indicate ground surface uplift; NA = Not available; ND = Not determined.

Table 7a: Corrected liquefaction-related ground surface subsidence for Patch A using LiDAR DEMs.

	Estimated Ground Surface Subsidence (mm)								
	10-m Buffer			20-m Buffer			50-m Buffer		
Earthquake Event(s)	16th %ile	50th %ile	84th %ile	16th %ile	50th %ile	84th %ile	16th %ile	50th %ile	84th %ile
Sep-10	<50	<50	50	<50	<50	50	<50	<50	50
Feb-11	50	50	50	50	50	50	50	50	50
Jun-11	<50	<50	50	<50	<50	50	<50	<50	50
Dec-11	<50	<50	50	<50	<50	50	<50	<50	50
CES	150	150	150	150	150	150	150	150	150

Note: These percentiles are not the exact statistical measures; they indicate the spatial variability of ground surface subsidence.

Table 7b: Corrected liquefaction-related ground surface subsidence for Road using LiDAR DEMs.

	Estimated Ground Surface Subsidence (mm)								
	10-m Buffer			20-m Buffer			50-m Buffer		
Earthquake Event(s)	16th %ile	50th %ile	84th %ile	16th %ile	50th %ile	84th %ile	16th %ile	50th %ile	84th %ile
Sep-10	NA	NA	NA	<50	<50	50	<50	<50	50
Feb-11	NA	NA	NA	50	100	100	50	100	100
Jun-11	NA	NA	NA	<50	<50	100	<50	<50	100
Dec-11	NA	NA	NA	<50	<50	50	<50	<50	50
CES	NA	NA	NA	150	150	250	150	150	250

Note: These percentiles are not the exact statistical measures; they indicate the spatial variability of ground surface subsidence.

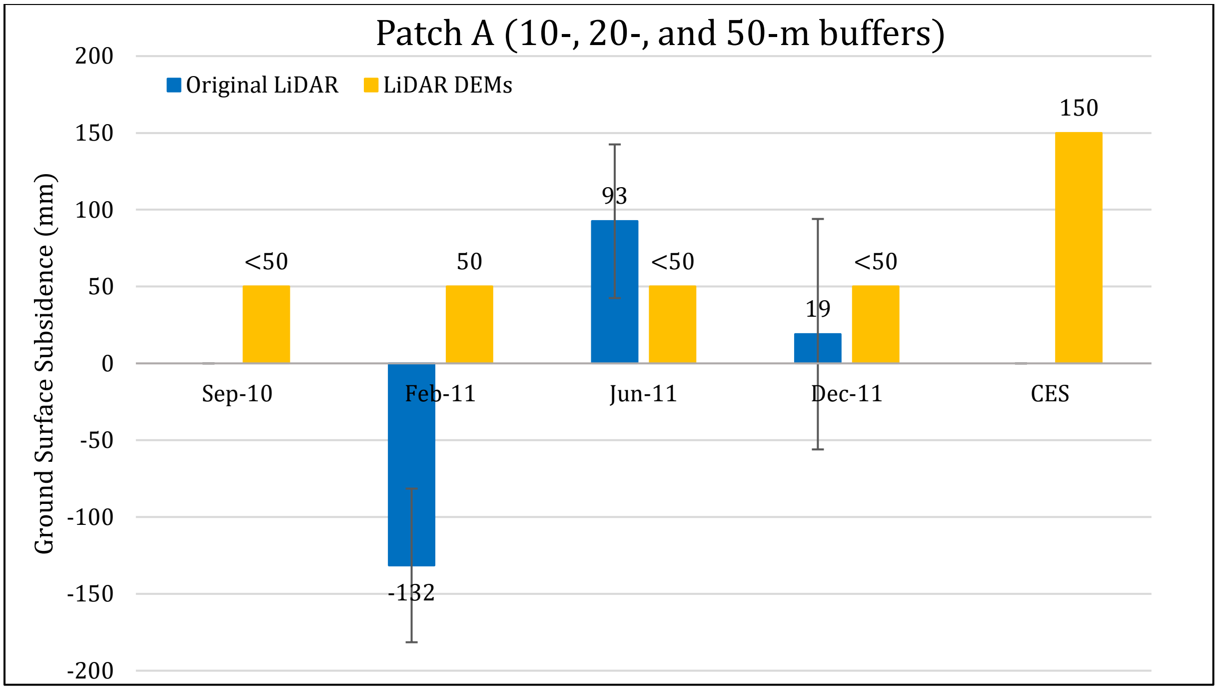

Figure 2: Comparison between ground surface subsidence determined from original LiDAR survey points and ground surface subsidence (50th %ile) estimated using LiDAR DEMs for Patch A.

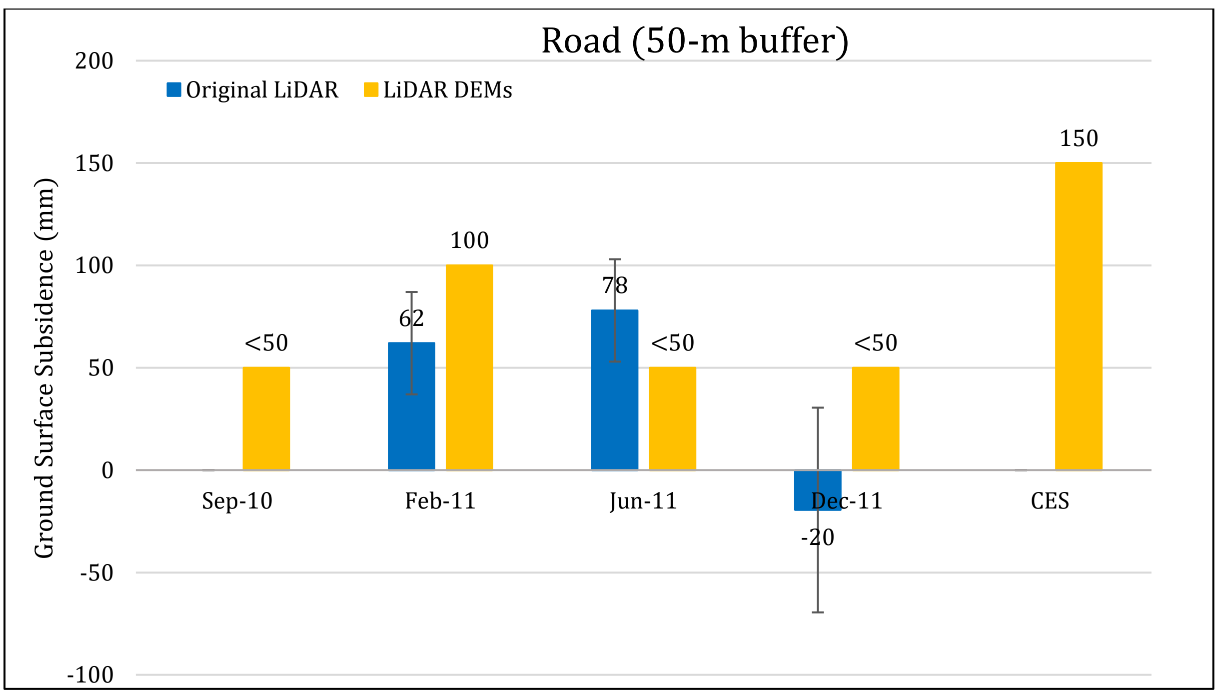

Figure 3: Comparison between ground surface subsidence determined from original LiDAR survey points and ground surface subsidence (50th %ile) estimated using LiDAR DEMs for Road (50-m buffer).

Note 2: The ground surface subsidence values determined from the original LiDAR survey points are similar to the ground surface subsidence values estimated using the LiDAR DEMs. The exception to this trend occurs for the Feb-11 EQ for Patch A as the ground surface subsidence computed using the original LiDAR survey points is -132 mm compared to 50 mm determined using the LiDAR DEM. One of the potential reasons for this discrepancy can be anthropogenic changes (e.g., land resurfacing) that might have occurred between the July 2003 and Sep 2010 LIDAR surveys but could not be seen in the available satellite images.

Table 8a: Ejecta-Induced settlement for the top 20 m of the soil profile for Patch A for the 50th %ile PGA, P_L=50%, and C_{FC}=0.13 using BI-2014, ZRB-2002, and I_C cutoff of 2.6.

Earthquake Event(s)	M_W	PGA (g)	Depth to Groundwater (m)	S_T (mm)	S_{V1D} (mm)	$S_{E,L}$ (mm)
Sep-10	7.1	0.18	1.6	ND	12±20	ND
Feb-11	6.2	0.49	1.4	-132±50	94±50	-226±71
Jun-11	6.2	0.23	1.3	93±50	17±25	76±56
Dec-11	6.1	0.36	0.9	19±75	57±50	-38±90

Notes: S_T = Total settlement (Table 6); S_{V1D} = Average vertical settlement due to volumetric compression using Boulanger and Idriss (2014) (BI-2014), Zhang et al. (2002) (ZRB-2002) procedures and de Greef and Lengkeek (2018) thin-layer correction; $S_{E,L}$ = Ejecta-induced settlement as the difference between the LiDAR-based S_T and S_{V1D}.

Table 8b: Ejecta-Induced settlement for the top 20 m of the soil profile for Road (50-m buffer) for the 50th %ile PGA, P_L=50%, and C_{FC}=0.13 using BI-2014, ZRB-2002, and I_C cutoff of 2.6.

Earthquake Event(s)	M_W	PGA (g)	Depth to Groundwater (m)	S_T (mm)	S_{V1D} (mm)	$S_{E,L}$ (mm)
Sep-10	7.1	0.18	1.6	ND	16±20	ND
Feb-11	6.2	0.49	1.4	62±25	128±50	-66±56
Jun-11	6.2	0.23	1.3	78±25	27±25	51±35
Dec-11	6.1	0.36	0.9	-20±50	90±50	-110±71

Notes: S_T = Total settlement (Table 6); S_{V1D} = Average vertical settlement due to volumetric compression using Boulanger and Idriss (2014) (BI-2014), Zhang et al. (2002) (ZRB-2002) procedures and de Greef and Lengkeek (2018) thin-layer correction; $S_{E,L}$ = Ejecta-induced settlement as the difference between the LiDAR-based S_T and S_{V1D}.

Note 3: The uncertainty for volumetric settlement was derived based on the sensitivity of volumetric settlement to PGA, C_{FC}, and P_L for each earthquake event for VsVp 57203 *Shirley Intermediate School* and CC LIQ 1 – CPT 5586 – *Vivian St* sites. Taking the 50th percentile as the baseline case, the minimum and maximum values corresponding to the difference between the 25th percentile and the 50th percentile and the 75th percentile and the 50th percentile were determined. The arithmetic mean of the range of the minimum and maximum difference was evaluated for each patch at the two sites.

The maximum arithmetic mean for each earthquake event was rounded to the nearest five and used as the uncertainty value. Accordingly, the 1-D volumetric settlement uncertainties of ±20, ±50, ±25, and ±50 mm for the Sep-10, Feb-11, Jun-11, and Dec-11 earthquake events, respectively, were used for all sites in this study.

Table 9a: Coverage area and height of ejecta estimates for Patch A using photographs.

EQ Event	$H_{E,thick1}$ (mm)	$A_{E,thick1}$ (m^2)	$H_{E,thick2}$ (mm)	$A_{E,thick2}$ (m^2)	$H_{E,thin1}$ (mm)	$A_{E,thin1}$ (m^2)	$H_{E,thin2}$ (mm)	$A_{E,thin2}$ (m^2)	A_T (m^2)
Sep-10	0	0	0	0	0	0	0	0	62.5
Feb-11	100-200	20.8	80-160	12.9	60-120	2.0	30-50	26.8	62.5
Jun-11	NA	NA	NA	NA	NA	NA	NA	NA	62.5
Dec-11	0	0	60-80	3.9	30-60	13.1	10-20	4.0	62.5

Notes: $A_{E,thin/thick}$ = Coverage area of thin/thick ejecta layers; $H_{E,thin/thick}$ = Lower-upper estimate of height of thin/thick ejecta layers; A_T= Total assessment area of a buffer being considered.

Table 9b: Coverage area and height of ejecta estimates for Road (50-m buffer) using photographs.

EQ Event	$H_{E,prism/pyr}$ (mm)	$V_{E,prism+pyr}$ (m^3)	$H_{E,thick}$ (mm)	$A_{E,thick}$ (m^2)	$H_{E,thin}$ (mm)	$A_{E,thin}$ (m^2)	A_T (m^2)
Sep-10	0	0	0	0	0	0	1291
Feb-11	11-135	5.10-10.2	5-10	16.3	2-4	144	1291
Jun-11	22-150	1.38-2.67	0	0	3-6	70.0	1170*
Dec-11	11-71	0.26-0.52	0	0	3-6	61.7	1291

Notes: $H_{E,prism/pyr}$ = Lower-upper estimate of ejecta height near the curb based on 2-4% cross slope of normal crown; $V_{E,prism+pyr}$ = Lower-upper estimate of total volume of prismatic- and pyramidal-shape ejecta; $A_{E,thin/thick}$ = Coverage area of thin/thick ejecta layers; $H_{E,thin/thick}$ = Lower-upper estimate of height of thin/thick ejecta layers; A_T = Total assessment area of a buffer being considered; * indicates reduction in A_T due to the presence of objects/shadows.

Note 4: The values in Table 9 correspond to the coverage area of ejecta outlined in aerial photographs (Figures 10, 11, 26, 28, and 63-65) and the lower and upper estimates of ejecta height based on geometrical approximations, ground photographs (Figures 67 and 68), and EQC LDAT property inspection reports (e.g., Figure 66). The ejecta-induced settlement using photographs and engineering judgment, $S_{E,P}$, is estimated as

$$S_{E,P} = \frac{\sum_{i=1}^{a} A_{E,thick,i} * H_{E,thick,i} + \sum_{j=1}^{b} A_{E,thin,j} * H_{E,thin,j} + \frac{1}{2}\sum_{n=1}^{f} W_{E,prism,n} * H_{E,prism,n} * L_{E,prism,n}}{A_T} + \frac{\frac{1}{3}\sum_{p=1}^{g} W_{E,r.pyramid,p} * H_{E,r.pyramid,p} * L_{E,r.pyramid,p}}{A_T} + \frac{\frac{1}{6}\sum_{r=1}^{h} W_{E,t.pyramid,r} * H_{E,t.pyramid,r} * L_{E,t.pyramid,r}}{A_T} = \frac{\sum_{i=1}^{a} V_{E,thick,i} + \sum_{j=1}^{b} V_{E,thin,j} + \sum_{n=1}^{f} V_{E,prism,n} + \sum_{p=1}^{g} V_{E,r.pyramid,p} + \sum_{r=1}^{h} V_{E,t.pyramid,r}}{A_T}$$

where

- $A_{E,thick,i}$ and $H_{E,thick,i}$ are the area and the height of a thick ejecta layer, respectively;
- $A_{E,thin,j}$ and $H_{E,thin,j}$ are the area and the height of a thin ejecta layer, respectively;
- $W_{E,prism,n}$ and $L_{E,prism,n}$ are the width and the length of the coverage area of a prismatically shaped ejecta layer, respectively, and $H_{E,prism,n}$ is the height of a prism-like ejecta layer;
- $W_{E,r.pyr,p}$ and $L_{E,r.pyr,p}$ are the width and the length, respectively, of the coverage area of an ejecta layer shaped as a pyramid with the rectangular base, and $H_{E,r.pyr,p}$ is the height of a rectangular-base pyramid-like ejecta layer;
- $W_{E,t.pyr,r}$ and $L_{E,t.pyr,r}$ are the width and the length, respectively, of the coverage area of an ejecta layer shaped as a pyramid with the triangular base, and $H_{E,t.pyr,p}$ is the height of a triangular-base pyramid-like ejecta layer;
- A_T is the total assessment area for a buffer being considered (Figure 1).

Table 10: Ejecta-induced settlement estimates for Patch A and Road based on photographs.

Earthquake Event	Patch A (10-, 20-, and 50-m buffers)		Road (50-m buffer)	
	$S_{E,P,lower}$ (mm)	$S_{E,P,upper}$ (mm)	$S_{E,P,lower}$ (mm)	$S_{E,P,upper}$ (mm)
Sep-10	0	0	0	0
Feb-11	65	125	4	8
Jun-11	NA	NA	1	3
Dec-11	11	19	≈0	1

Note: $S_{E,P,lower}$ and $S_{E,P,upper}$ correspond to lower and upper estimates of $S_{E,P}$, respectively.

Table 11: Best final estimates of ejecta-induced settlement for Patch A and Road.

Earthquake Event	Patch A (10-, 20-, and 50-m buffers)			Road (50-m buffer)		
	$S_{E,L}$ (mm)	$S_{E,P}$ (mm)	$S_{E,final}$ (mm)	$S_{E,L}$ (mm)	$S_{E,P}$ (mm)	$S_{E,final}$ (mm)
Sep-10	ND	0	0	ND	0	0
Feb-11	-226±71	95±30	95±30	-66±56	6±2	5±5
Jun-11	76±56	NA	*75±55	51±35	2±1	5±5
Dec-11	-38±90	15±4	15±5	-110±71	0.5±0.5	<5

Notes: $S_{E,L}$ = Ejecta-induced settlement based on LiDAR data reported in Table 8; $S_{E,P}$ = Median ejecta-induced settlement for the range of values reported in Table 10; $S_{E,final}$ = Best final estimate of ejecta-induced settlement rounded to the nearest 5 mm; Final plus/minus values are also rounded to the nearest 5 mm; ND = Not determined; * indicates uncertainty in the estimate due to the lack of physical evidence.

Note 5:

- Patch A: $S_{E,final}$ for the Sep-10, Feb-11, and Dec-11 EQs is based solely on $S_{E,P}$ due to the evident absence of ejecta for the Sep-10 EQ and the negative $S_{E,L}$ values for the Feb-11 and Dec-11 EQs. $S_{E,final}$ for the Jun-11 EQ is based solely on $S_{E,L}$ due to the unavailability of $S_{E,P}$.
- Road: $S_{E,final}$ for the $S_{E,P}$ for the Sep-10, Feb-11, and Dec-11 EQs is based solely on $S_{E,P}$ due to the evident absence of ejecta for the Sep-10 EQ and the negative $S_{E,L}$ values for the Feb-11 and Dec-11 EQs. $S_{E,final}$ for the Jun-11 EQ is a weighted average of $S_{E,L}$ and $S_{E,P}$ with the weight coefficients of 0.1 and 0.9, respectively. The uncertainty for $S_{E,final}$ is also a weighted average of the uncertainties associated with $S_{E,L}$ and $S_{E,P}$ with the same respective weight coefficients of 0.1 and 0.9.
- The weight coefficients are based on the LiDAR error bands, LPI prediction error (Maurer et al. 2014[3]), presence of ejecta at the time of LiDAR surveys, density of July 2003 LiDAR points, completeness of visual evidence (i.e., ground and aerial photographs and EQC LDAT property inspection reports for the site), and obvious discrepancy between the LiDAR-based estimates of ejecta-induced settlement and the observed quantum of ejecta. The Palmers Rd site is in the apparent zone of higher ground surface subsidence for the Sep-10 EQ (i.e., the July 2003 LiDAR flight error). It is not in the apparent zone of lower ground surface subsidence for the Feb-11 EQ. The site is in the zone of accurate LPI prediction of liquefaction severity for the Sep-10 and Feb-11 EQ. The LDAT property inspection report and ground photographs showing ejecta remnants for the property with Patch A are available. The inspection team noted ejecta in the backyard and front yard and under the house; the maximum ejecta height was recorded as ~250 mm on 3 June 2011. Ejecta were also observed at other properties within the 50-m buffer; the ejecta height ranged from 100 mm to 300 mm on 3 June 2011. There are no ground photographs of ejecta on the road.

<u>Summary 1</u>:

- **The best estimate of the ejecta-induced free-field ground settlement at the Palmers Rd site for the SEP 2010, FEB 2011, JUN 2011, and DEC 2011 earthquake is 0 mm, 95±30 mm, 75±55 mm, and 15±5 mm, respectively. There is uncertainty in the ejecta-induced settlement estimate for the JUN 2011 earthquake due to the lack of visual evidence for Patch A; the provided value is based on the LiDAR data only.**
- **The best estimate of the ejecta-induced free-field ground settlement of the road at the Palmers Rd St site for the SEP 2010, FEB 2011, JUN 2011, and DEC 2011 earthquake is 0 mm, 5±5 mm, 5±5 mm, and <5 mm, respectively.**

[3] Maurer, B. W., Green, R. A., Cubrinovski, M., & Bradley, B. A. (2014). Evaluation of the Liquefaction Potential Index for Assessing Liquefaction Hazard in Christchurch, New Zealand. *Journal of Geotechnical and Geoenvironmental Engineering*, 140(7), 04014032-1-11. doi:10.1061/(asce)gt.1943-5606.0001117

Figure 4: Location of the site.

Figure 5: Position of the site relative to nearby free-face features.

Figure 6: Position of the site relative to nearby buildings and vegetation.

Figure 7: Street view of the flat land.

Figure 8: Satellite image of the site taken in Dec 2004.

Figure 9: Satellite image of the site taken in Mar 2009.

Figure 10: Satellite image of the site taken on Sep 3, 2010.

Figure 11: Satellite image of the site taken on Sep 5, 2010.

Figure 12: Satellite image of the site taken on Feb 7, 2011.

Figure 13: Satellite image of the site taken on Feb 23, 2011.

Figure 14: Satellite image of the site taken on Feb 26, 2011.

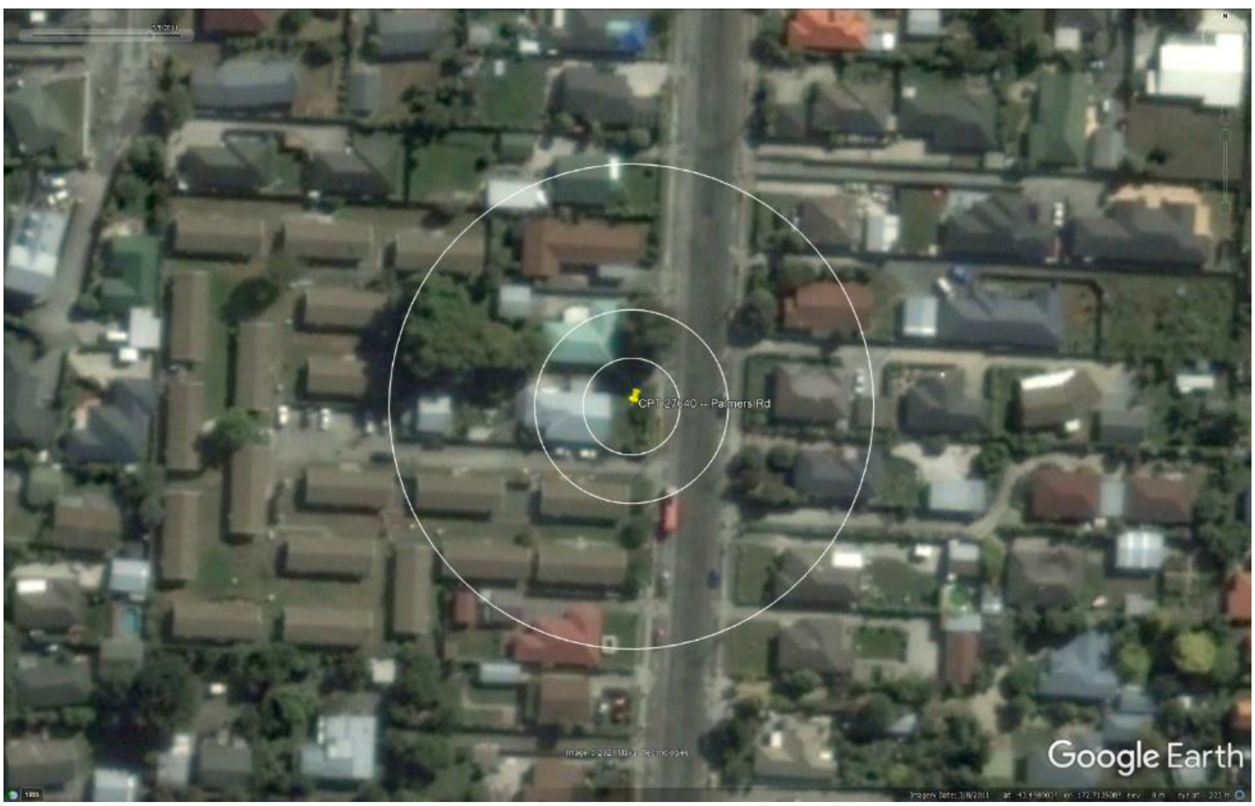

Figure 15: Satellite image of the site taken on Mar 8, 2011.

Figure 16: Satellite image of the site taken in Apr 2012.

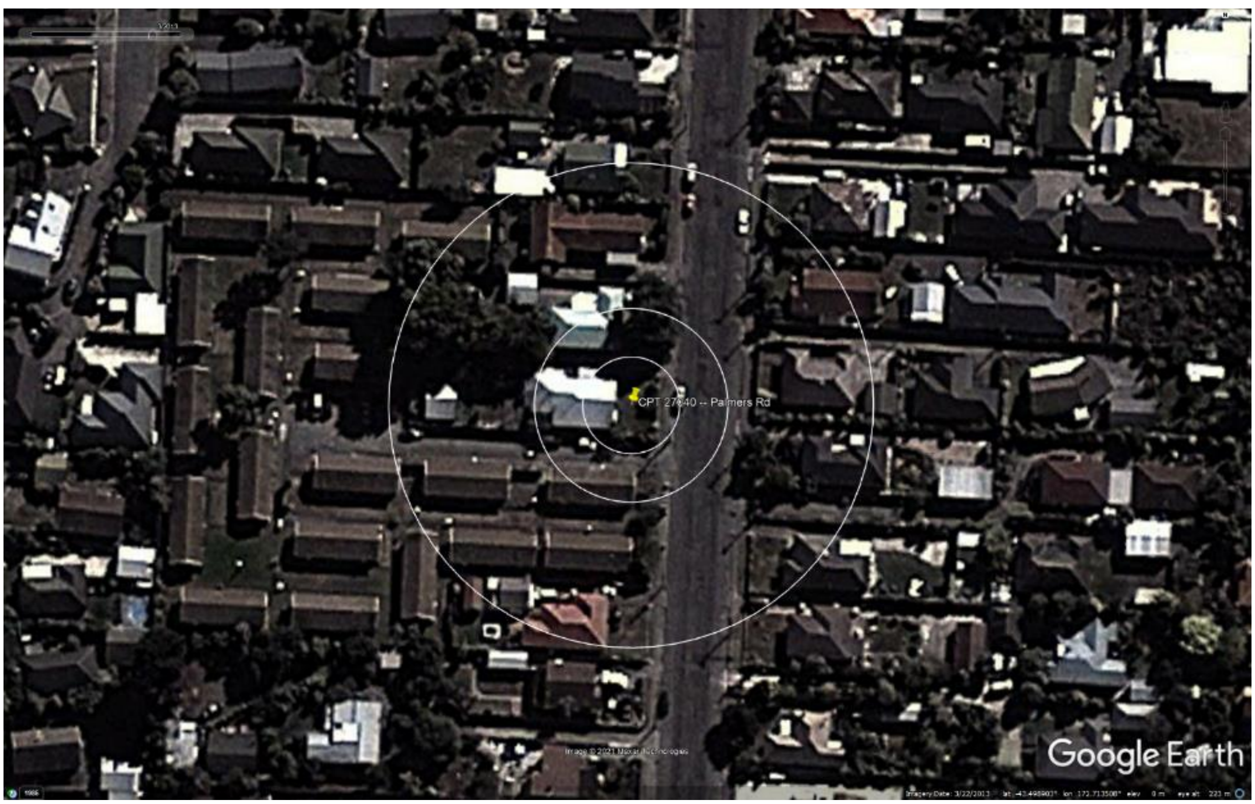

Figure 17: Satellite image of the site taken in Mar 2013.

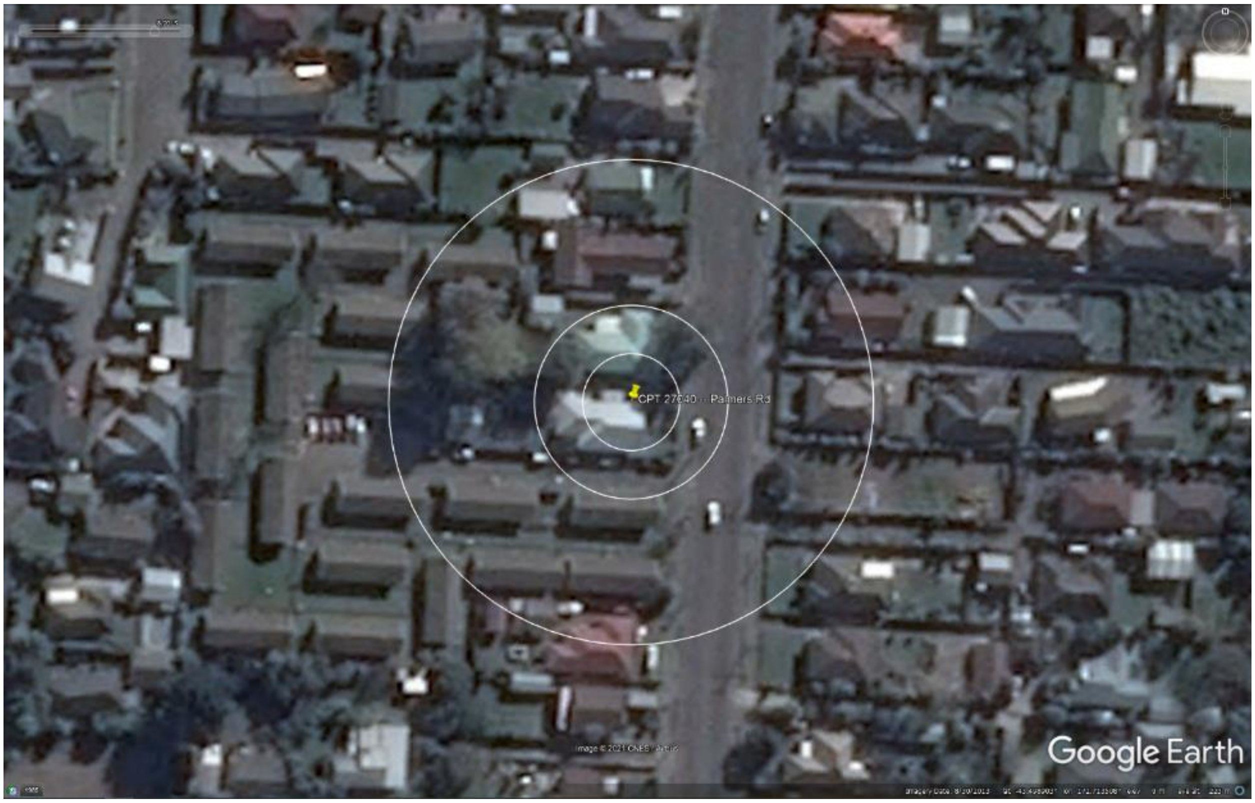

Figure 18: Satellite image of the site taken in Aug 2013.

Figure 19: Satellite image of the site taken in Sep 2013.

Figure 20: Satellite image of the site taken in Feb 2014.

Figure 21: Satellite image of the site taken in Aug 2014.

Figure 22: Satellite image of the site taken in Jan 2015.

Figure 23: Satellite image of the site taken in Apr 2015.

Figure 24: Satellite image of the site taken in Jun 2015.

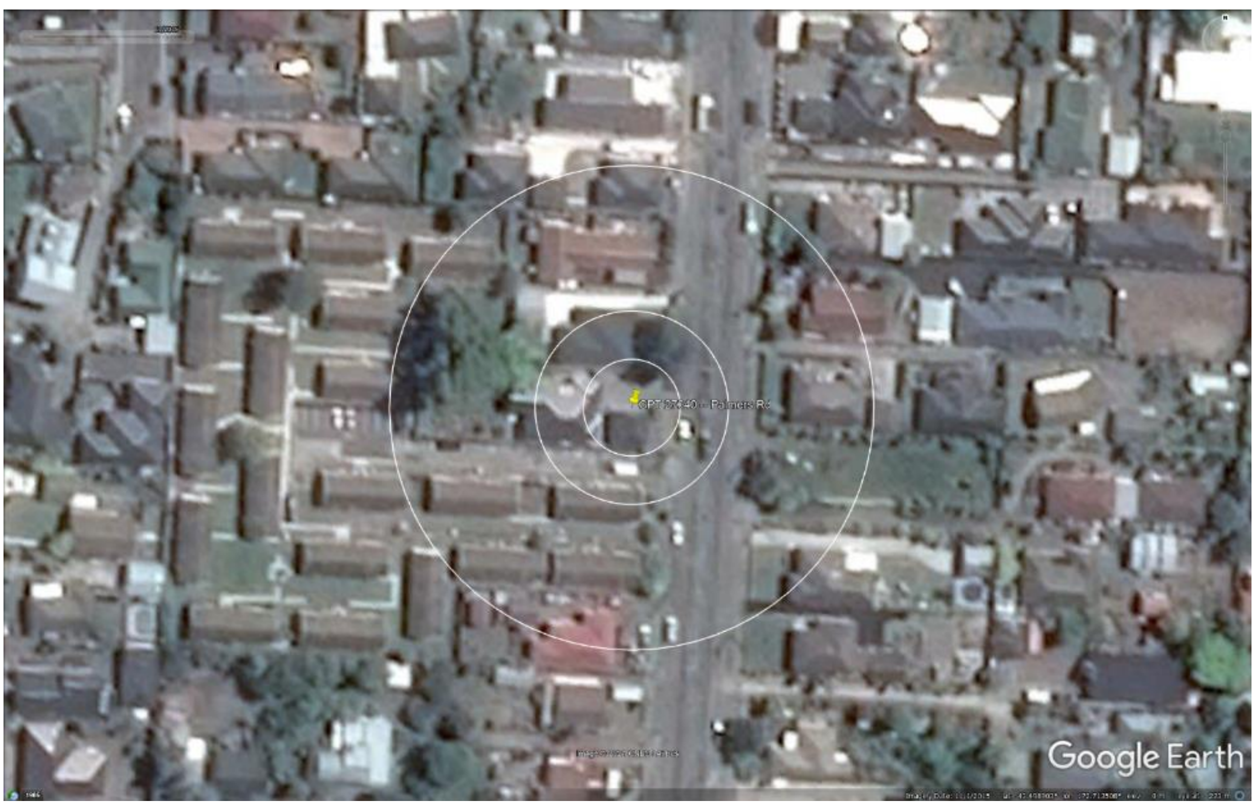

Figure 25: Satellite image of the site taken in Nov 2015.

Figure 26: Aerial photograph of the site taken on Sep 4, 2010.

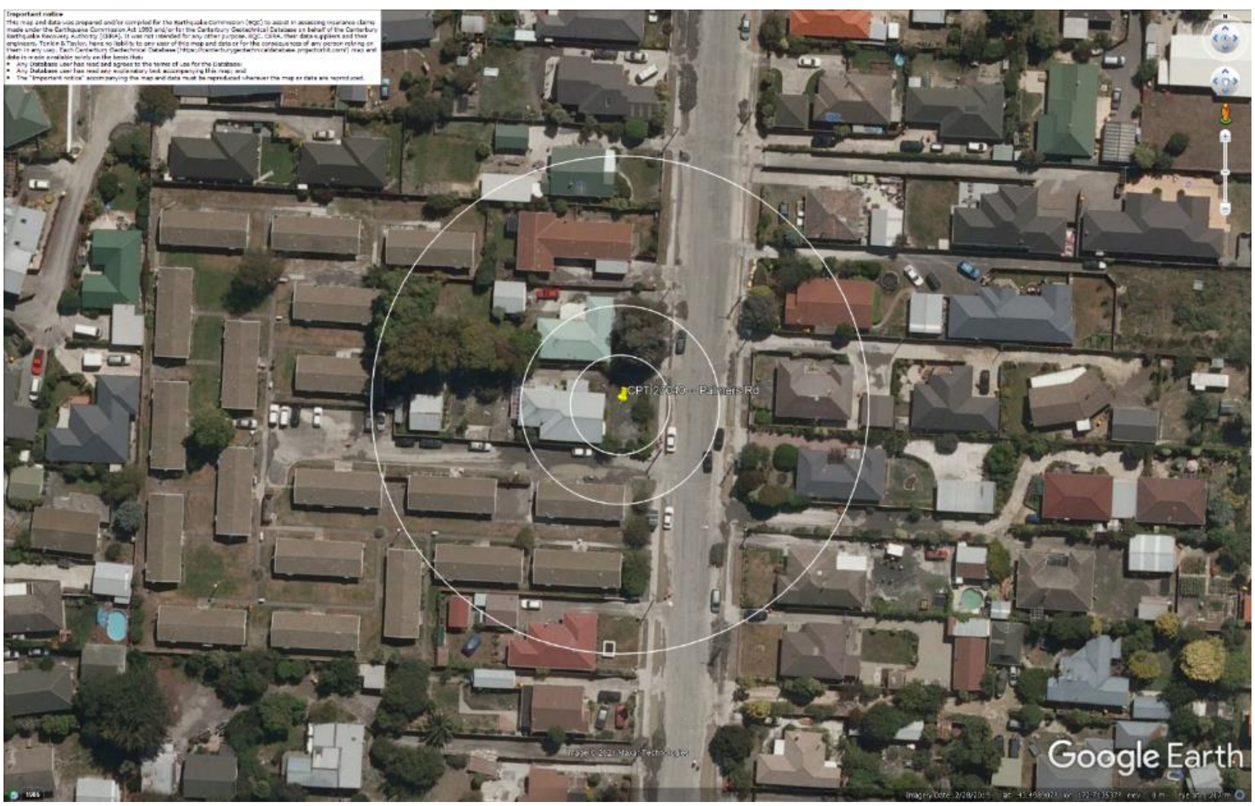

Figure 27: Aerial photograph of the site taken on Feb 24, 2011.

Figure 28: Aerial photograph of the site taken on June 14-15, 2011.

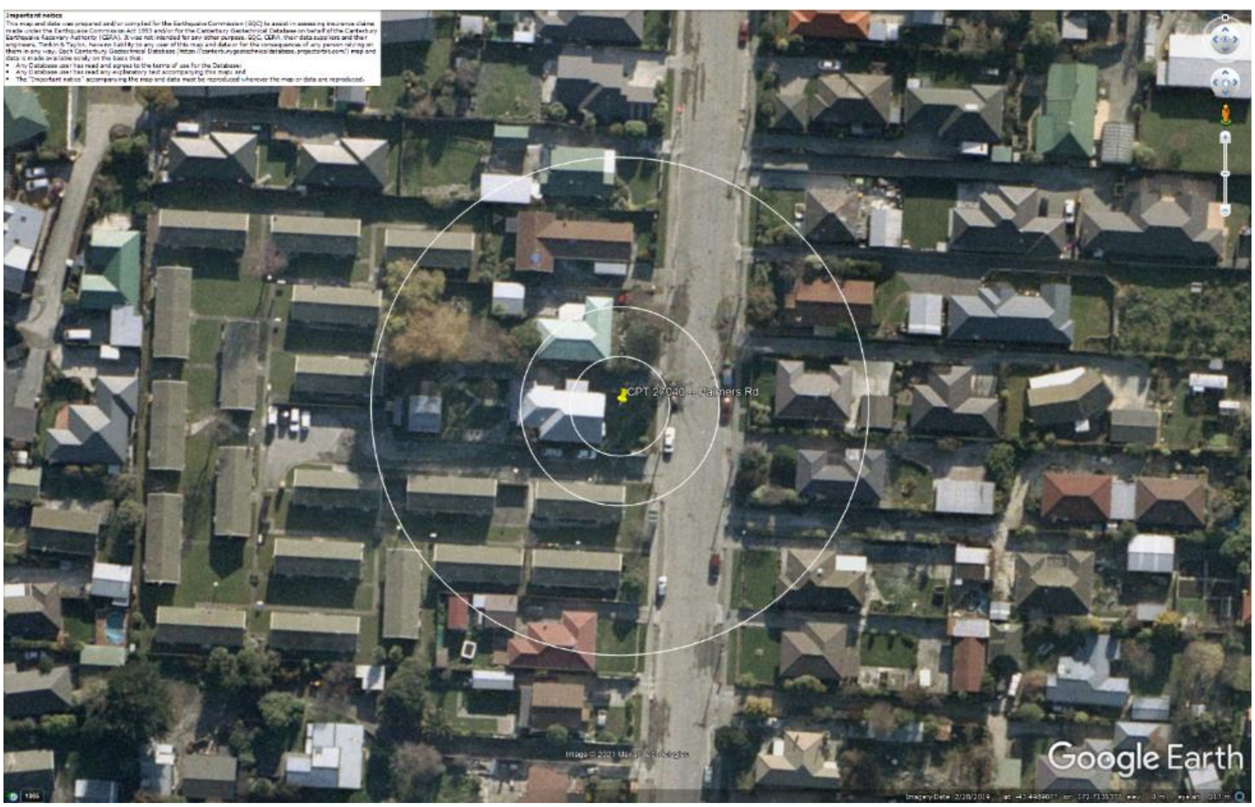

Figure 29: Aerial photograph of the site taken on June 16, 2011.

Figure 30: Aerial photograph of the site taken on Dec 24, 2011.

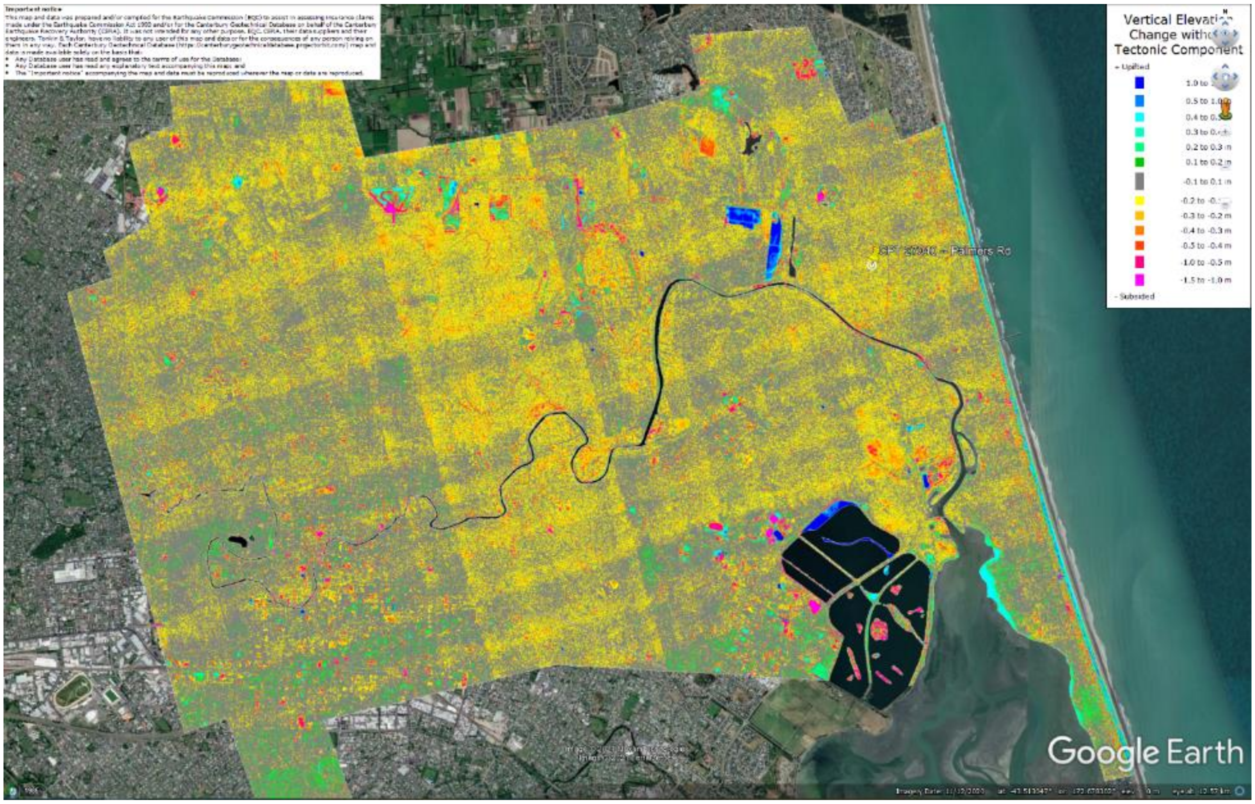

Figure 31: Vertical Ground Movements (Surface – Tectonic) for Sep 2010 Earthquake – the site is in the apparent zone of overestimated ground surface subsidence (i.e., July 2003 and Sep 2010 flight error bands).

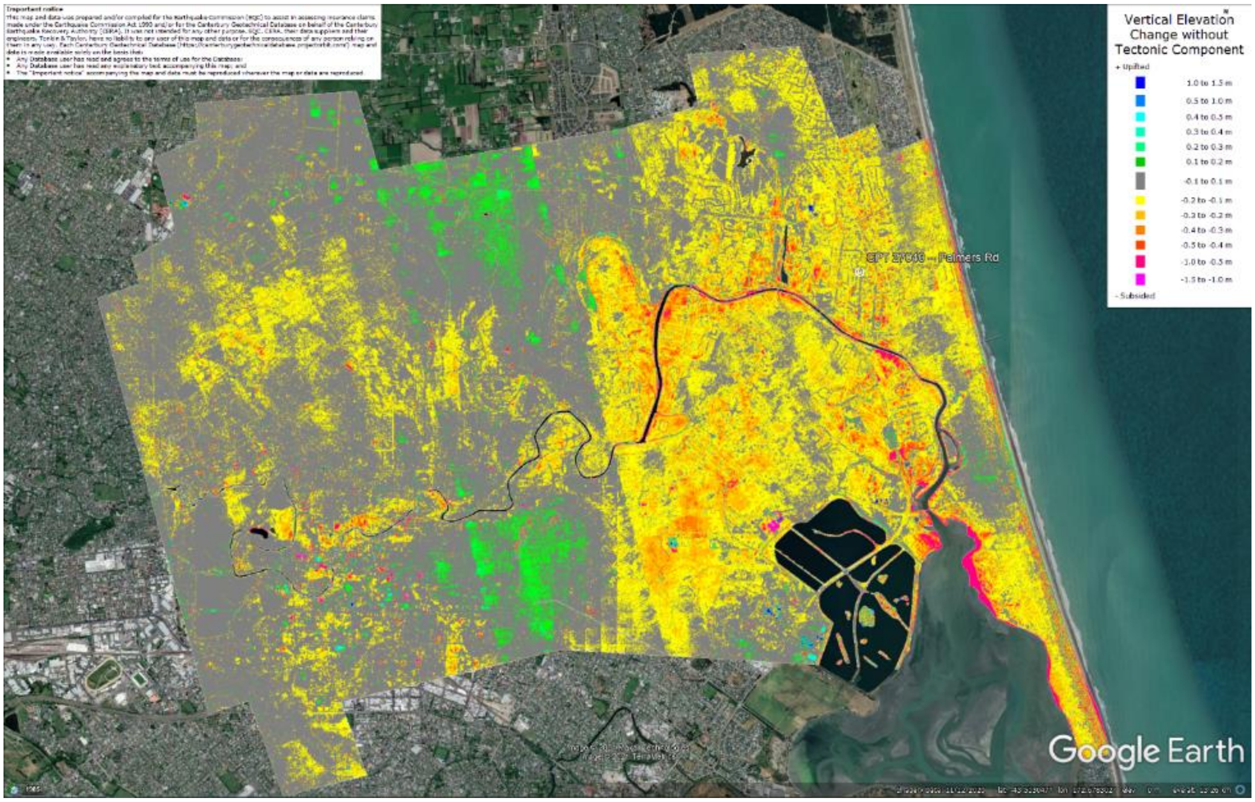

Figure 32: Vertical Ground Movements (Surface – Tectonic) for Feb 2011 Earthquake – the site is in the apparent zone of underestimated ground surface subsidence (e.g., Sep 2010 LiDAR flight error band).

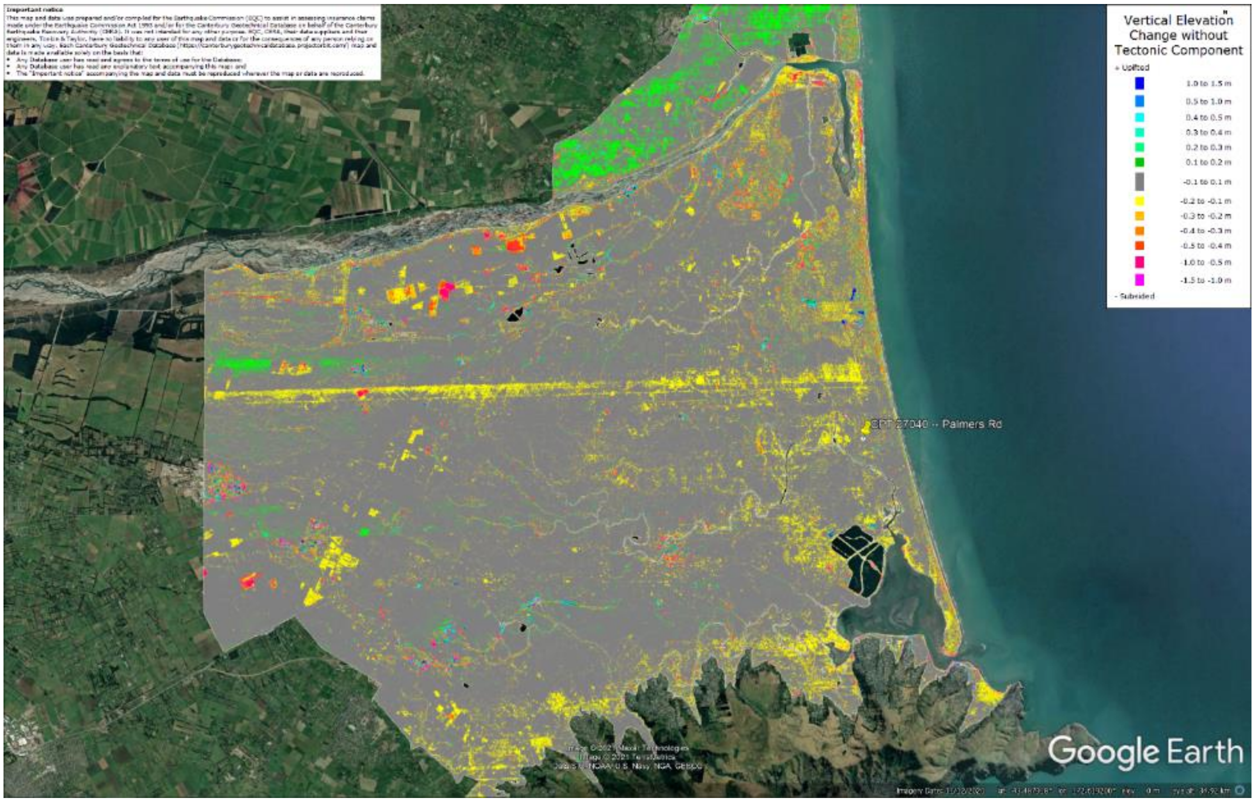

Figure 33: Vertical Ground Movements (Surface – Tectonic) for June 2011 Earthquake – the site is not in the apparent zone of overestimated or underestimated ground surface subsidence.

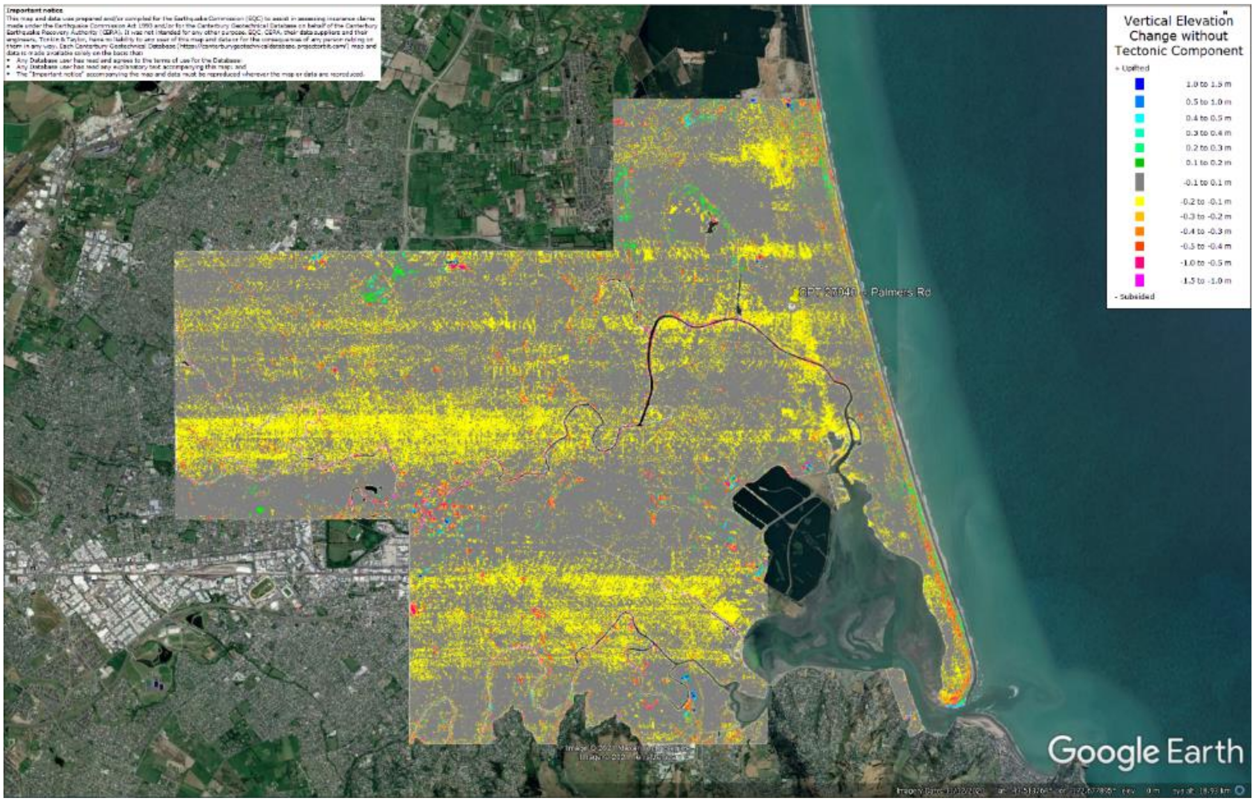

Figure 34: Vertical Ground Movements (Surface – Tectonic) for Dec 2011 Earthquake – the site is not in the apparent zone of overestimated or underestimated ground surface subsidence.

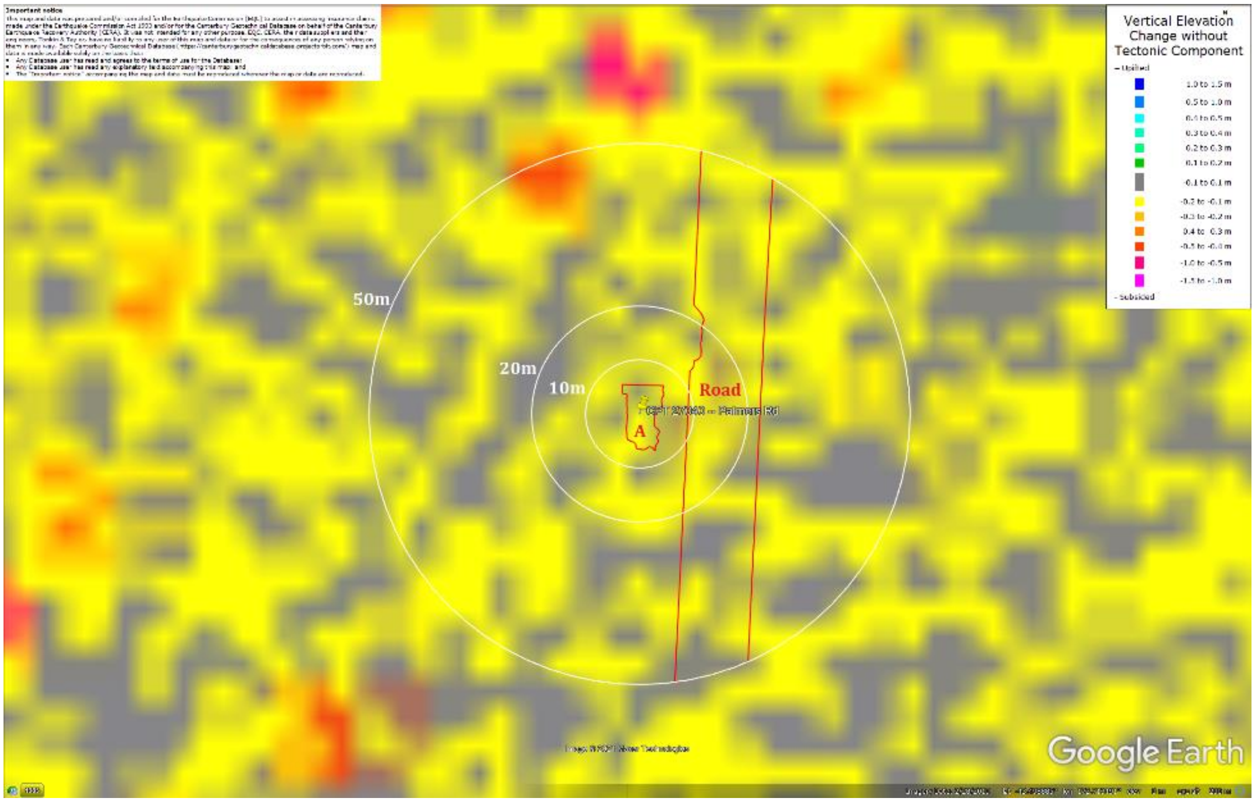

Figure 35: Ground surface subsidence without tectonic component for Sep 2010 Earthquake according to the LiDAR DEM.

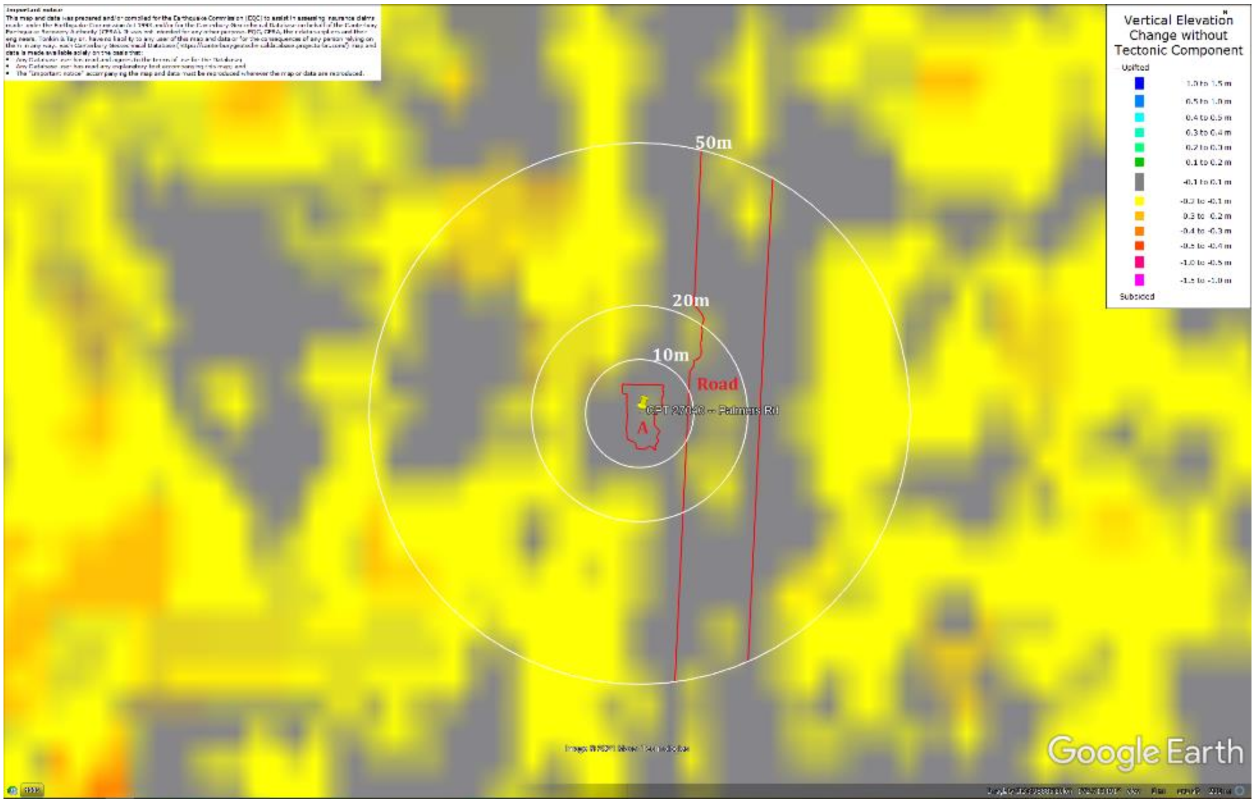

Figure 36: Ground surface subsidence without tectonic component for Feb 2011 Earthquake according to the LiDAR DEM.

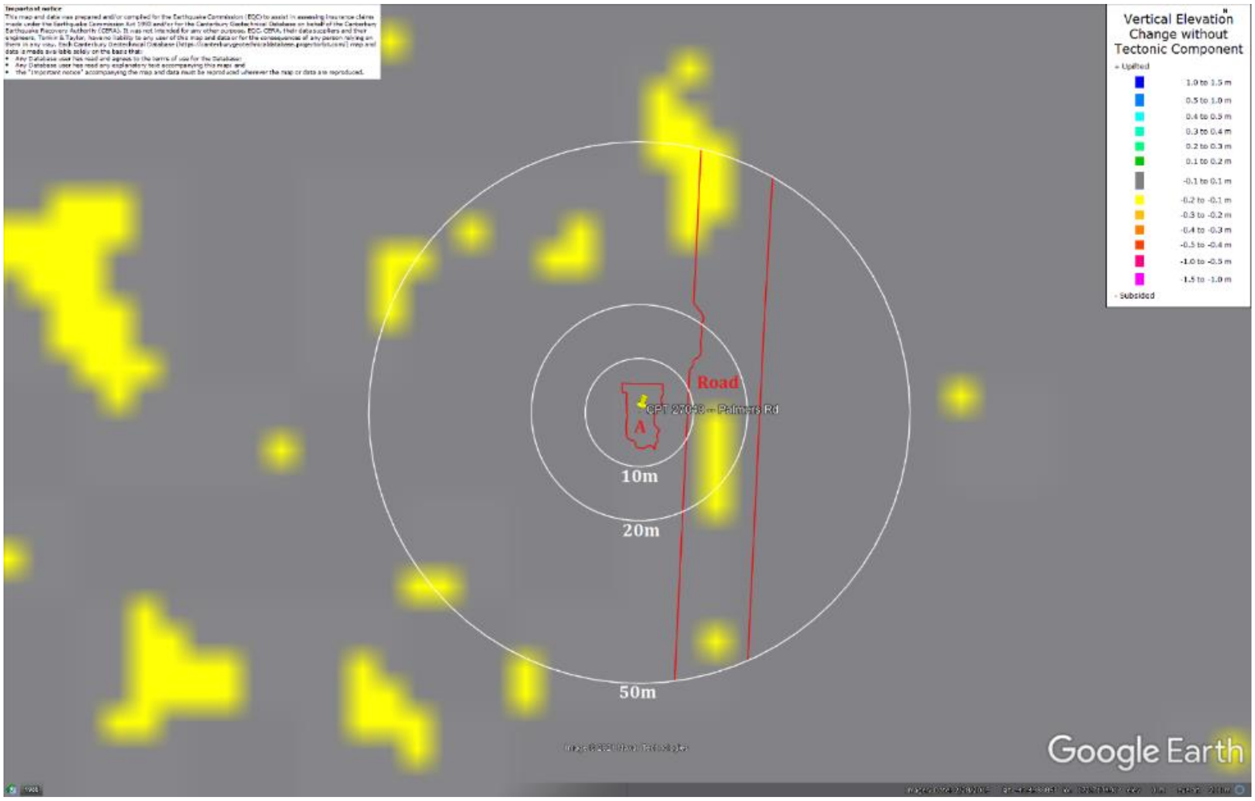

Figure 37: Ground surface subsidence without tectonic component for June 2011 Earthquake according to the LiDAR DEM.

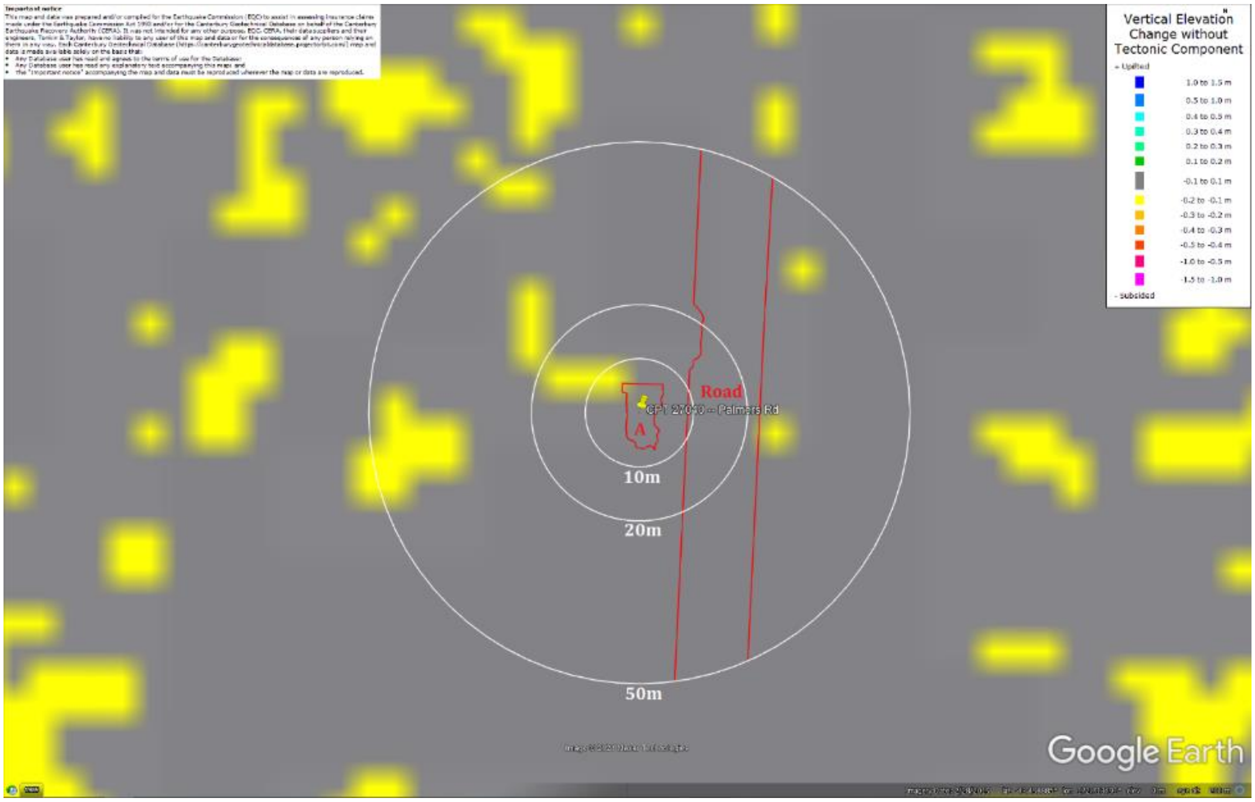

Figure 38: Ground surface subsidence without tectonic component for Dec 2011 Earthquake according to the LiDAR DEM.

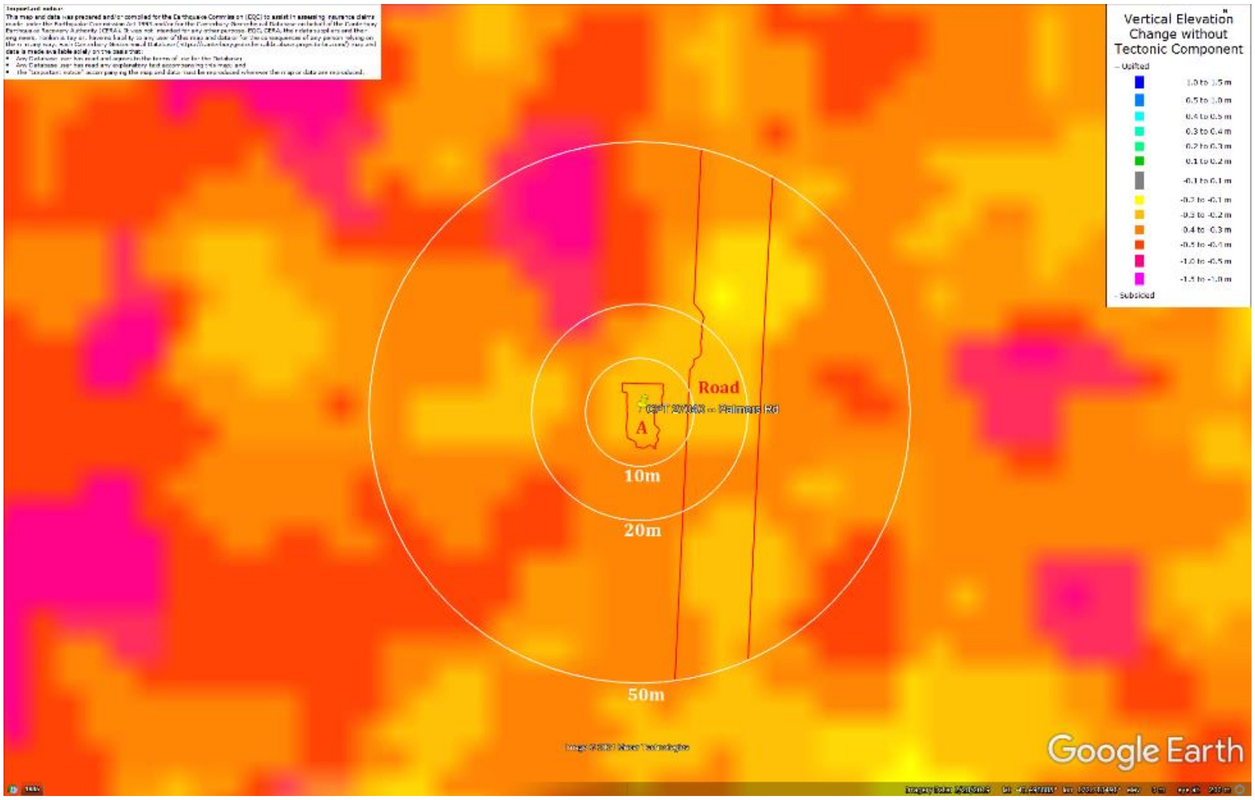

Figure 39: Ground surface subsidence without tectonic component for Canterbury Earthquake Sequence according to the LiDAR DEM.

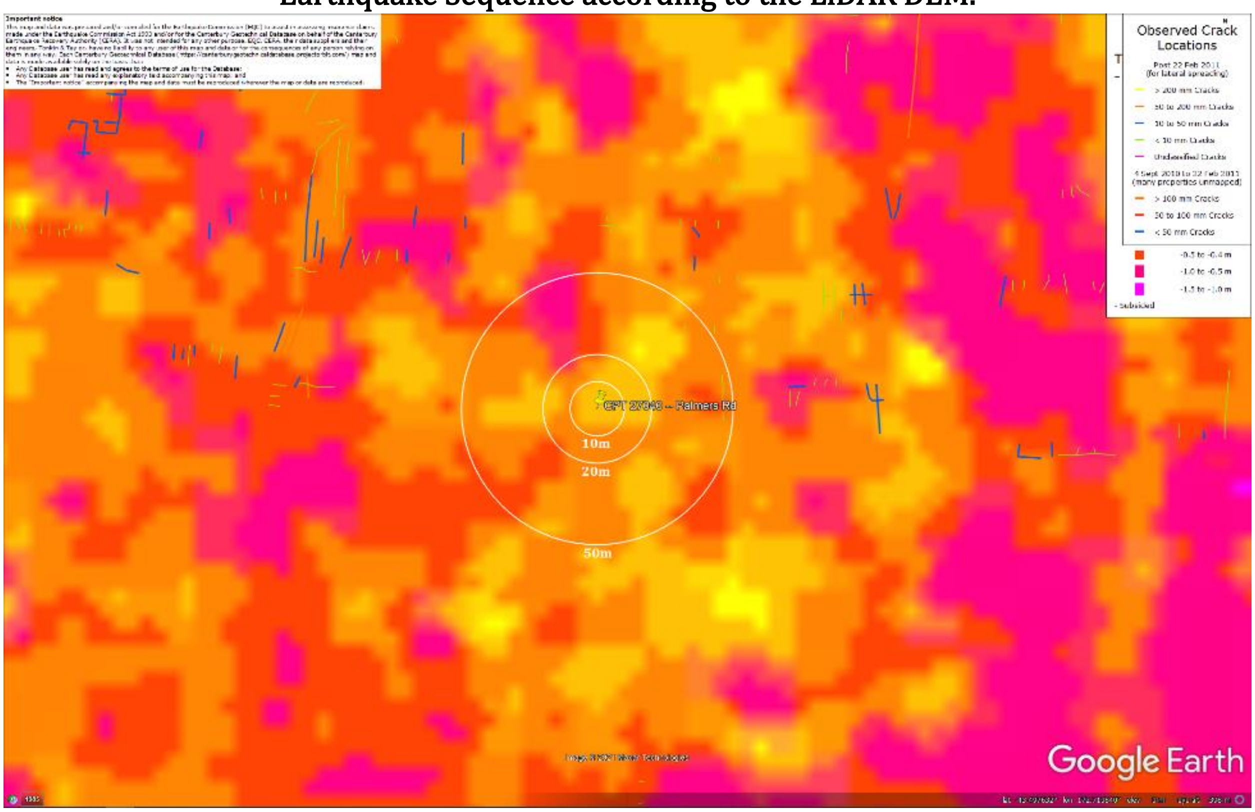

Figure 40: No lateral spreading for Canterbury Earthquake Sequence.

Figure 41: Vertical tectonic movements for Sep 2010 Earthquake.

Figure 42: Vertical tectonic movements for Feb 2011 Earthquake.

Figure 43: Vertical tectonic movements for June 2011 Earthquake.

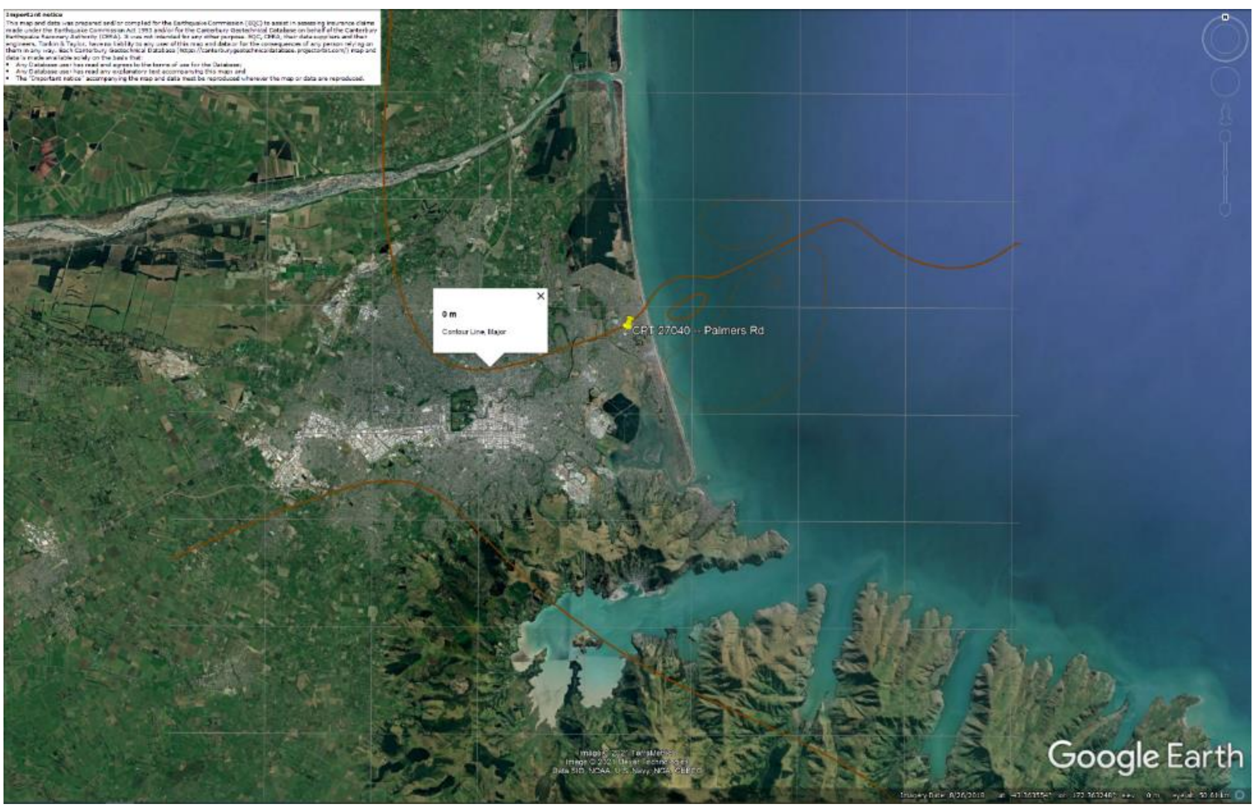

Figure 44: Vertical tectonic movements for Dec 2011 Earthquake.

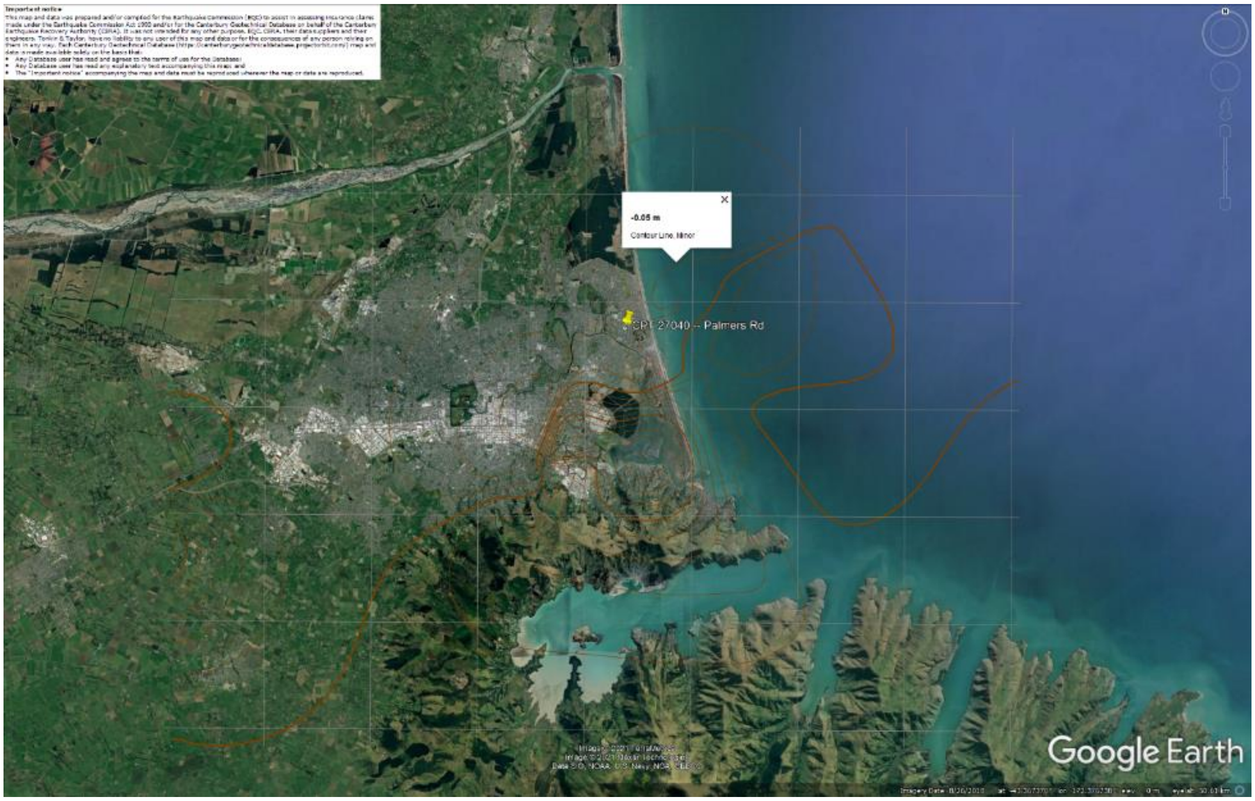

Figure 45: Vertical tectonic movements for Canterbury Earthquake Sequence.

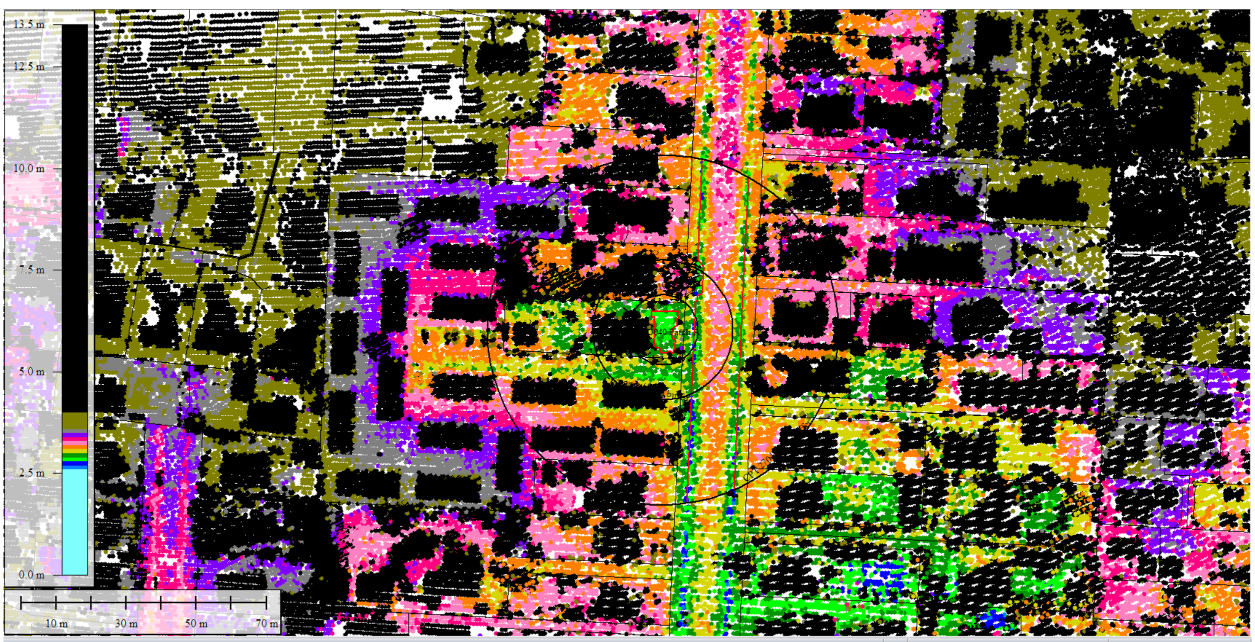

Figure 46: Sep 5, 2010 LiDAR survey.

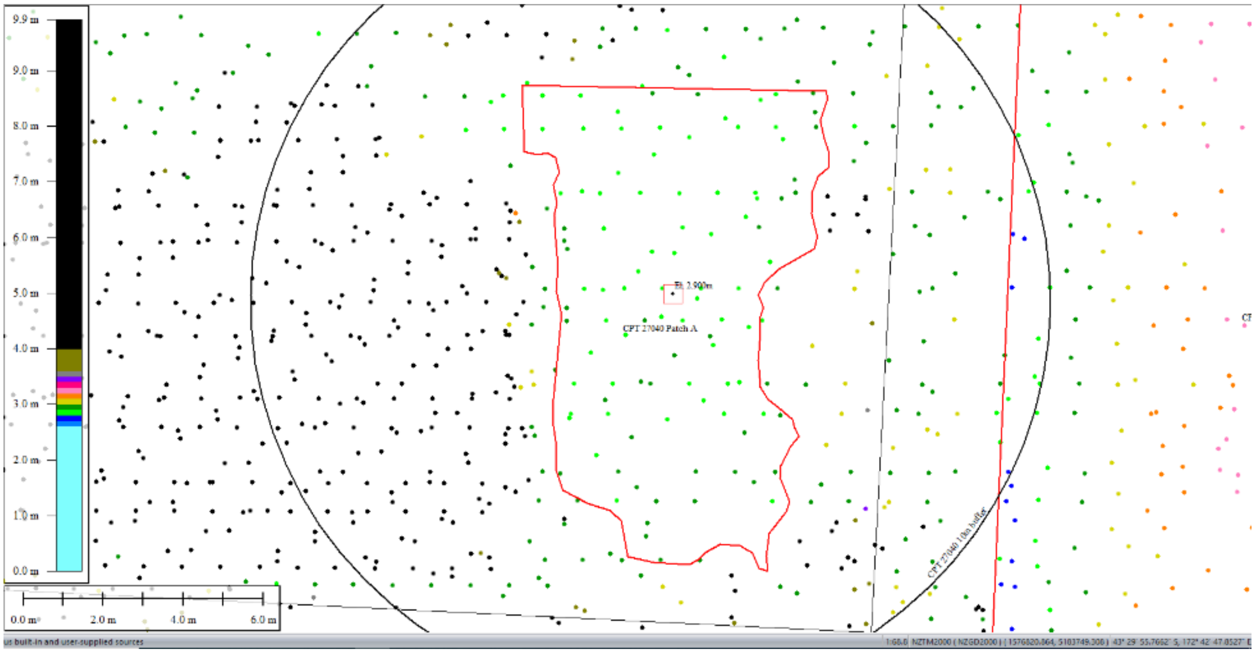

Figure 47: Ground surface elevation averaged over 10-m, 20-m, and 50-m buffers for Patch A for Sep 5, 2010 LiDAR survey.

Figure 48: Ground surface elevation averaged over 50-m buffer for Road for Sep 5, 2010 LiDAR survey.

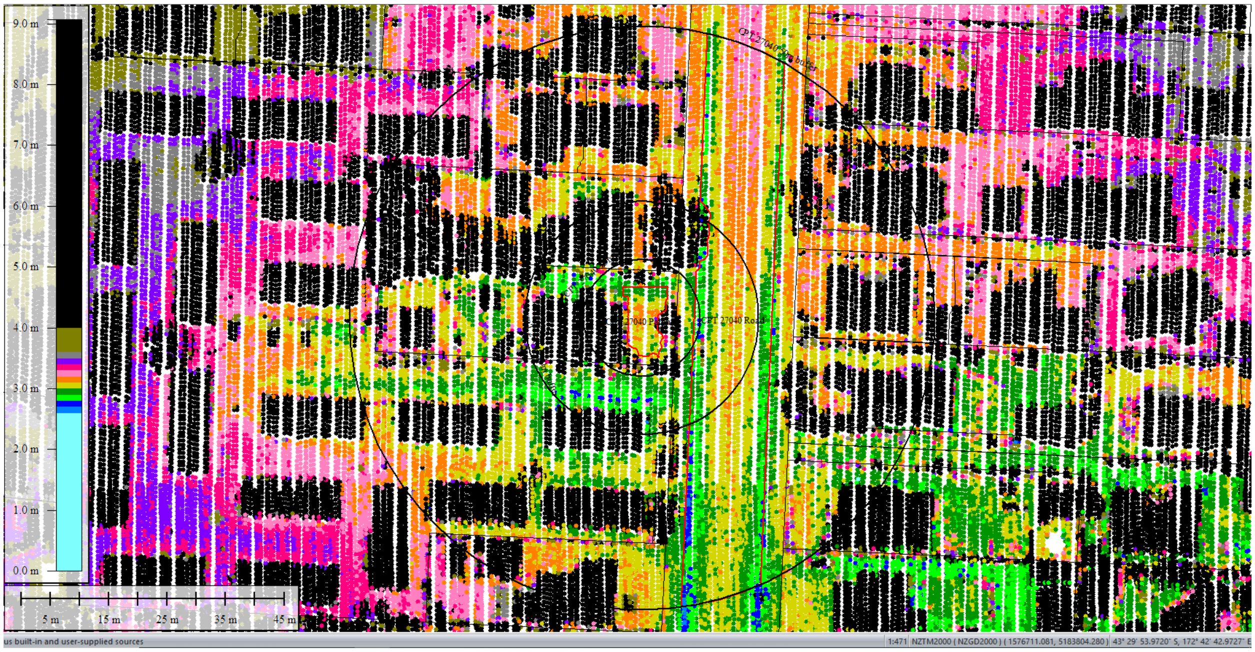

Figure 49: Mar 2011 LiDAR survey.

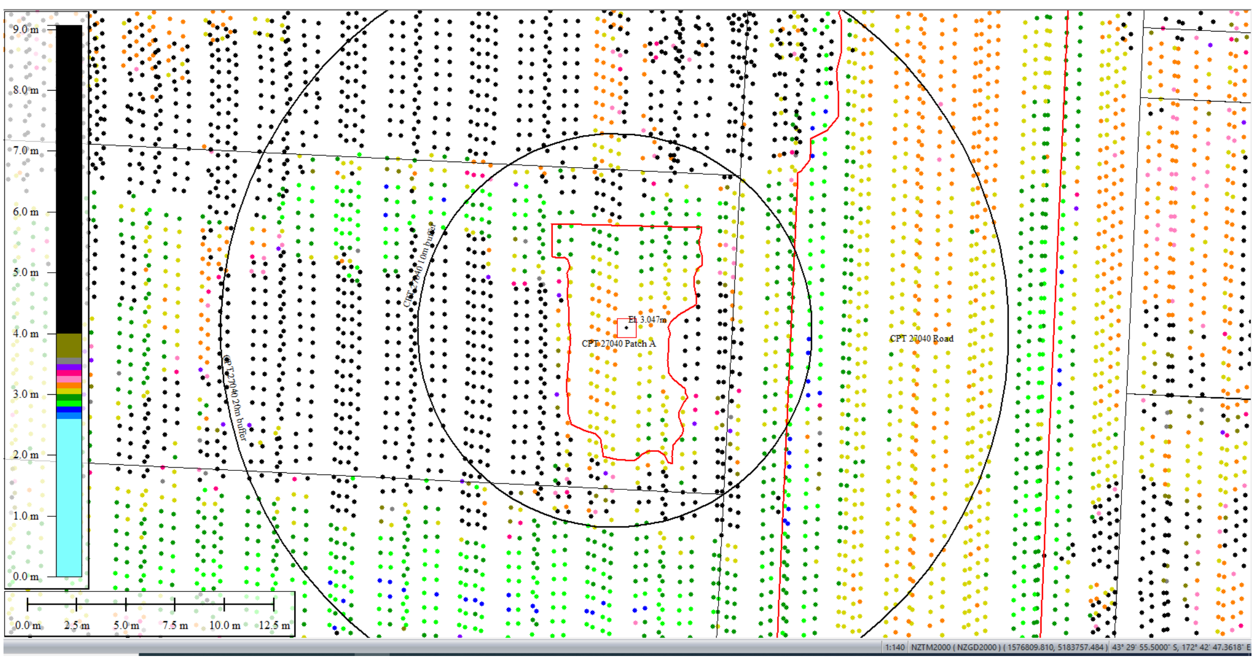

Figure 50: Ground surface elevation averaged over 10-m, 20-m, and 50-m buffers for Patch A for Mar 2011 LiDAR survey.

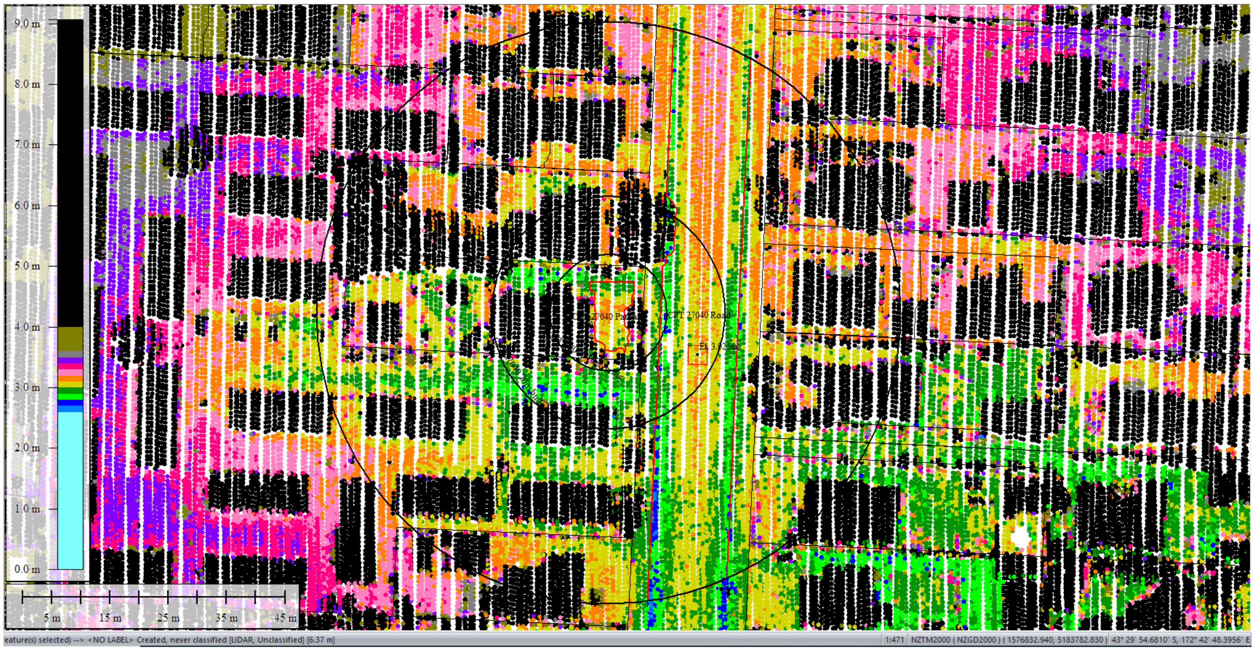

Figure 51: Ground surface elevation averaged over 50-m buffer for Road for Mar 2011 LiDAR survey.

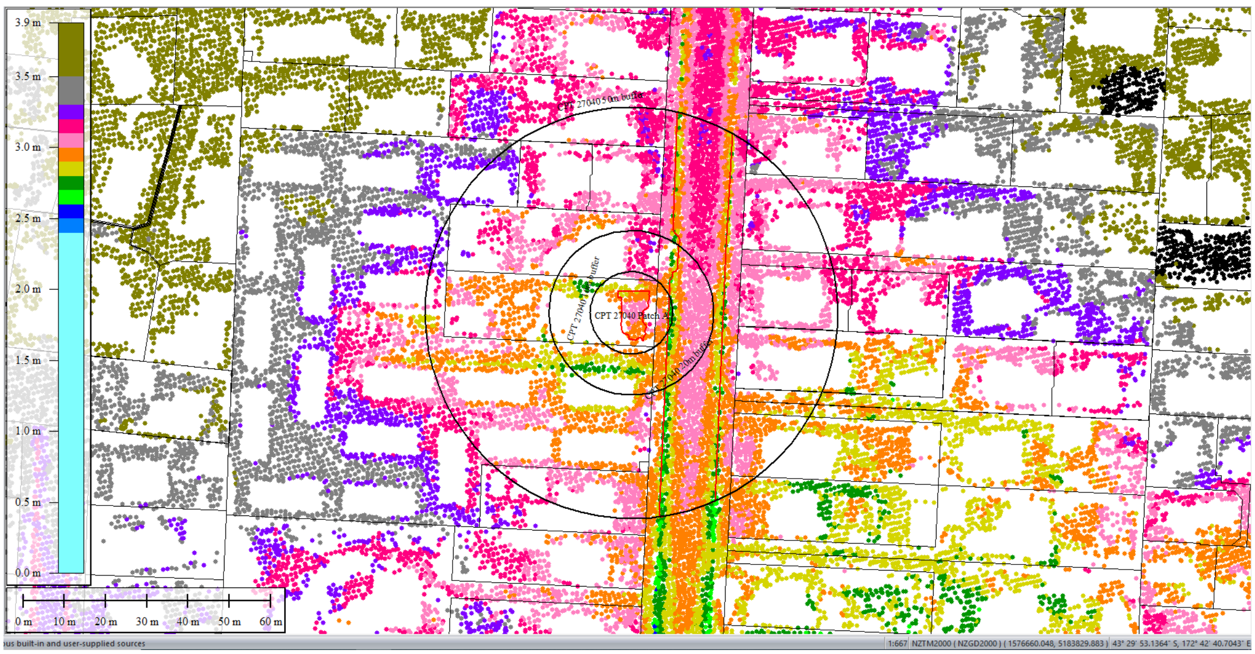

Figure 52: May 2011 LiDAR survey.

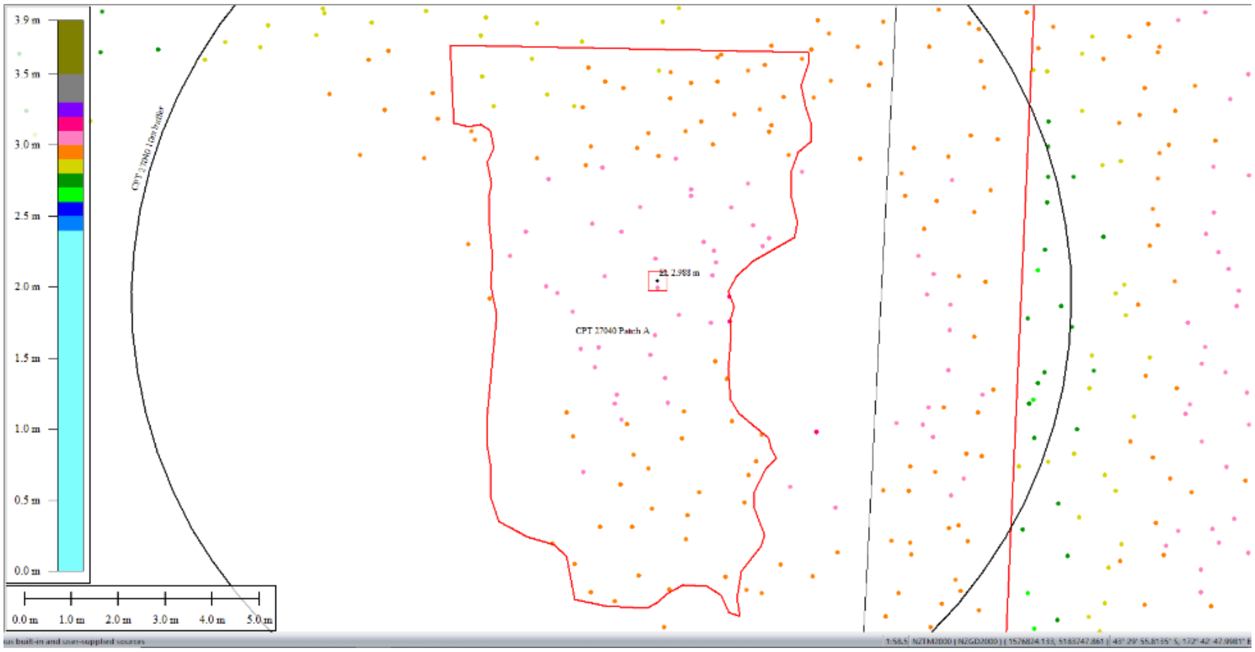

Figure 53: Ground surface elevation averaged over 10-m, 20-m, and 50-m buffers for Patch A for May 2011 LiDAR survey.

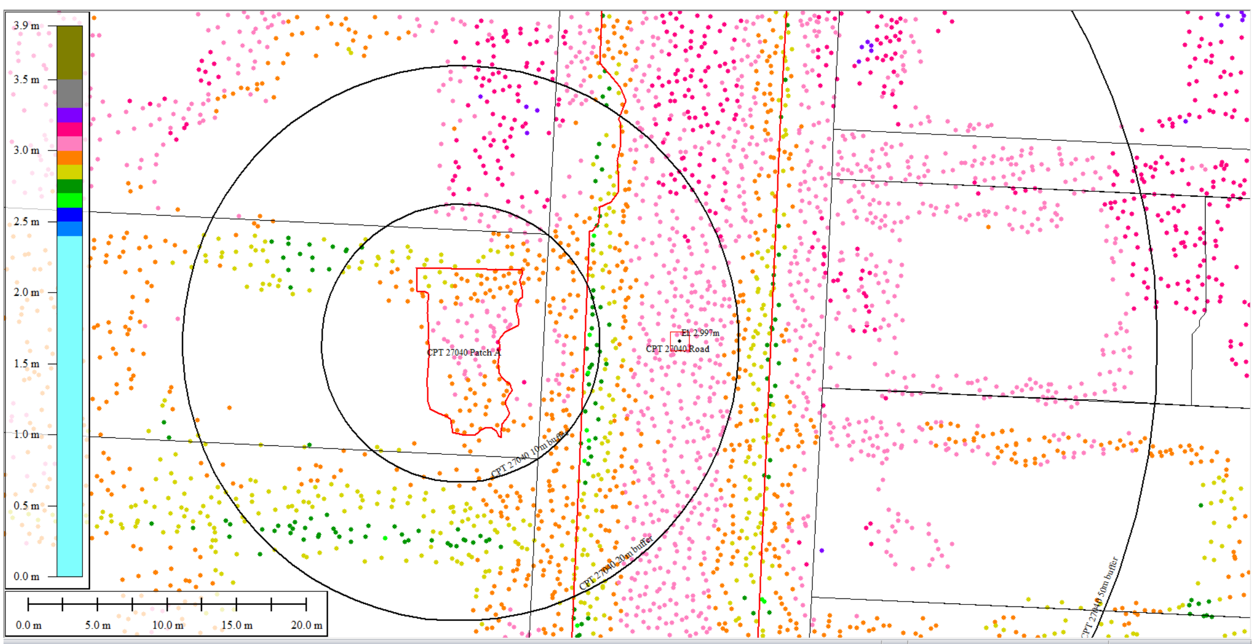

Figure 54: Ground surface elevation averaged over 50-m buffer for Road for May 2011 LiDAR survey.

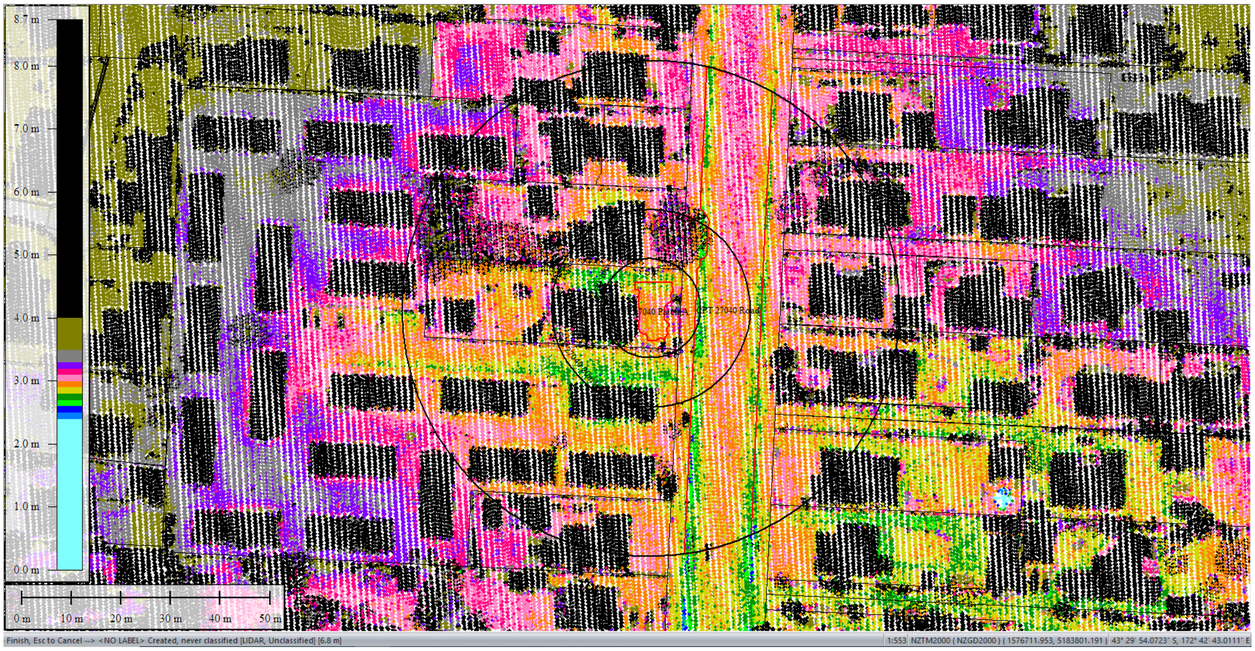

Figure 55: Sep 2011 LiDAR survey.

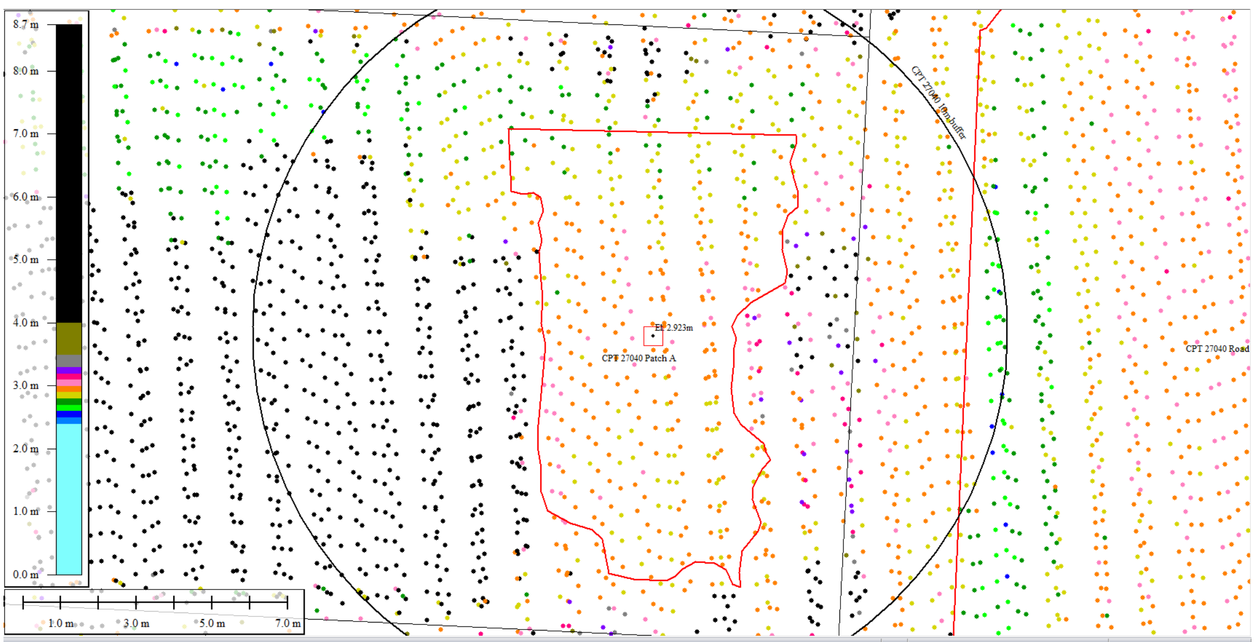

Figure 56: Ground surface elevation averaged over 10-m, 20-m, and 50-m buffers for Patch A for Sep 2011 LiDAR survey.

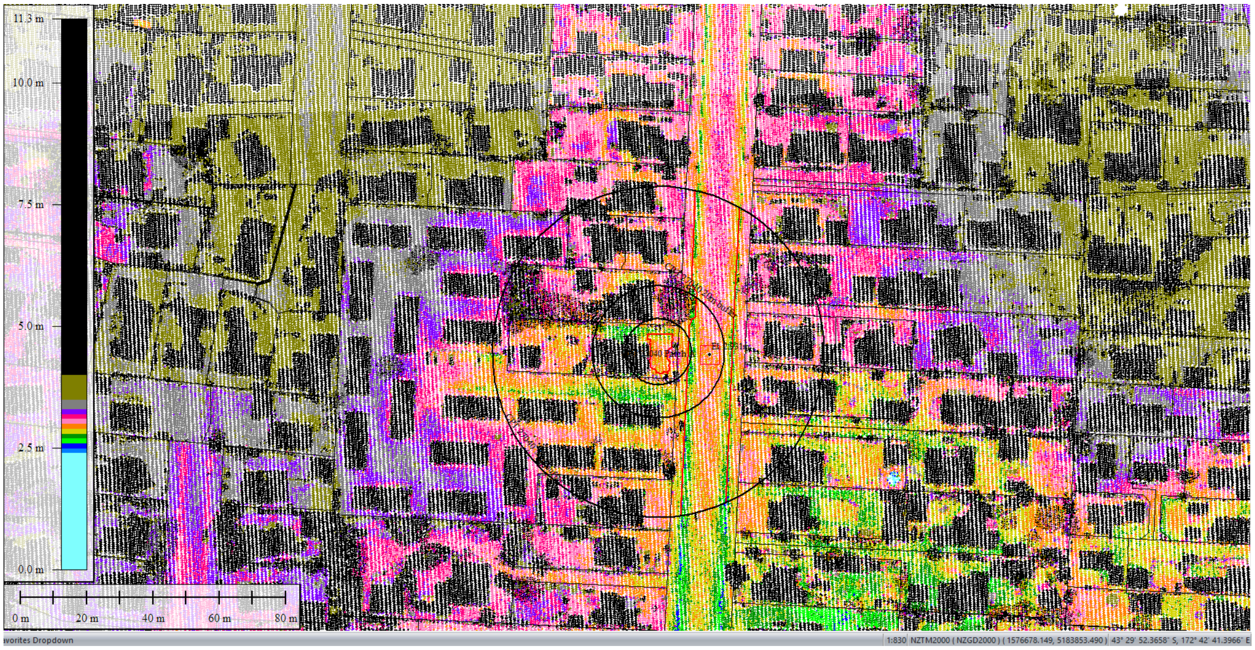

Figure 57: Ground surface elevation averaged over 50-m buffer for Road for Sep 2011 LiDAR survey.

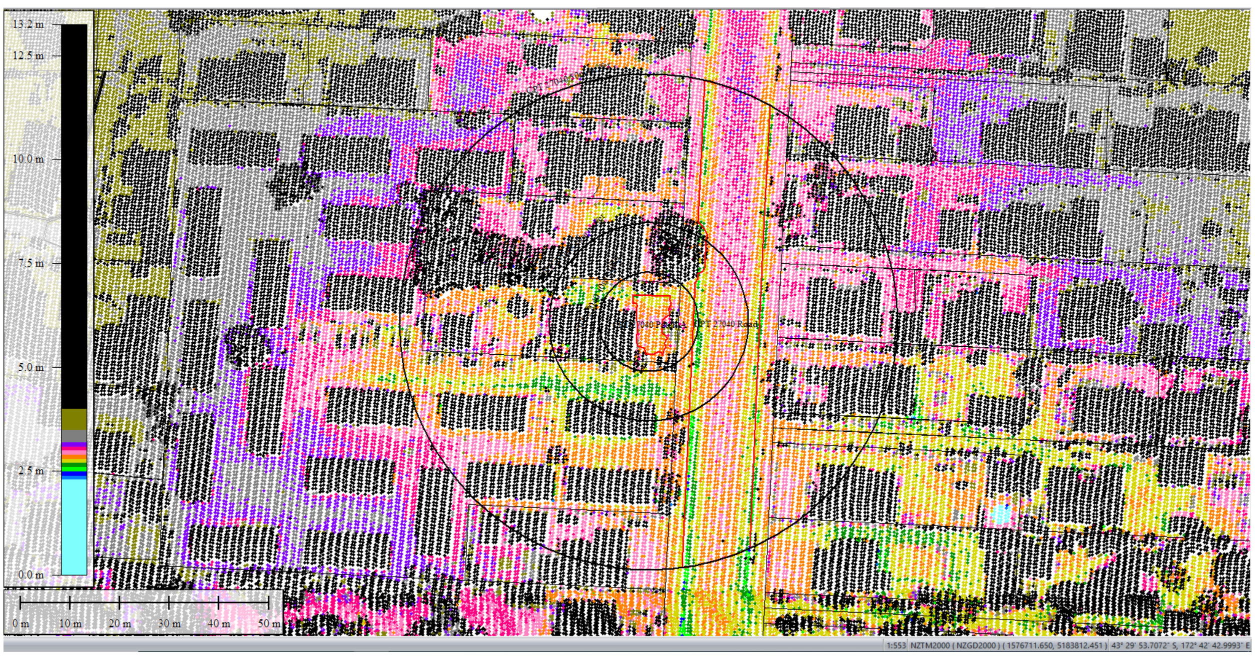

Figure 58: Feb 2012 LiDAR survey.

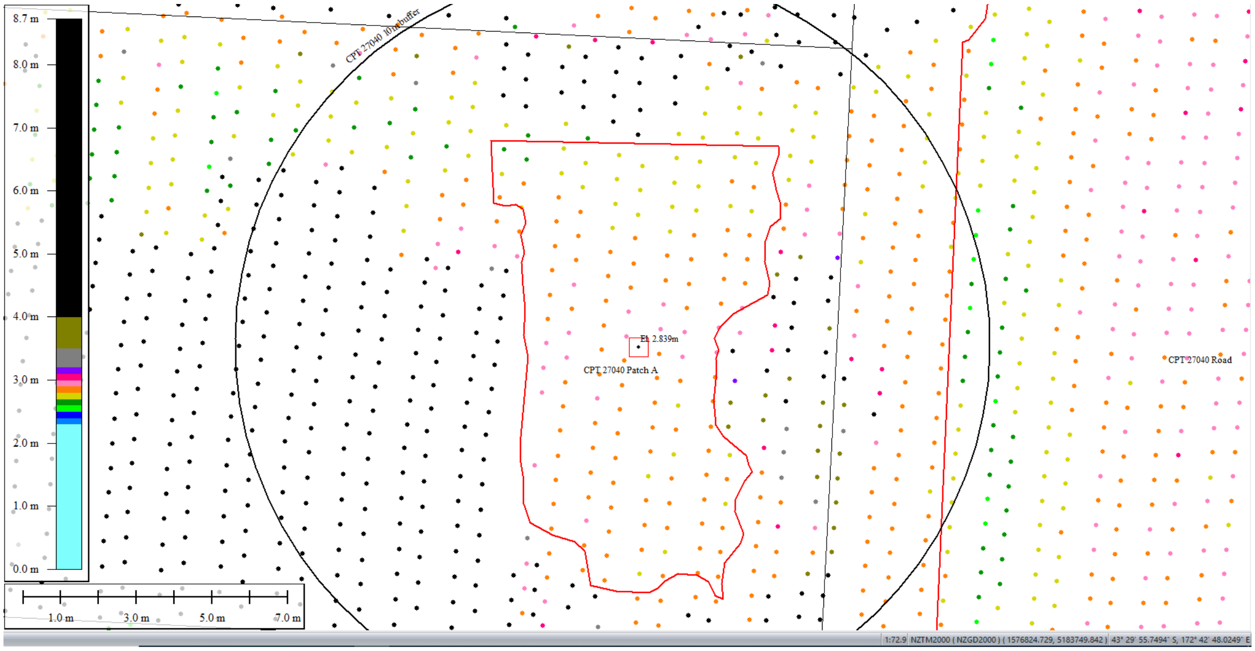

Figure 59: Ground surface elevation averaged over 10-m, 20-m, and 50-m buffers for Patch A for Feb 2012 LiDAR survey.

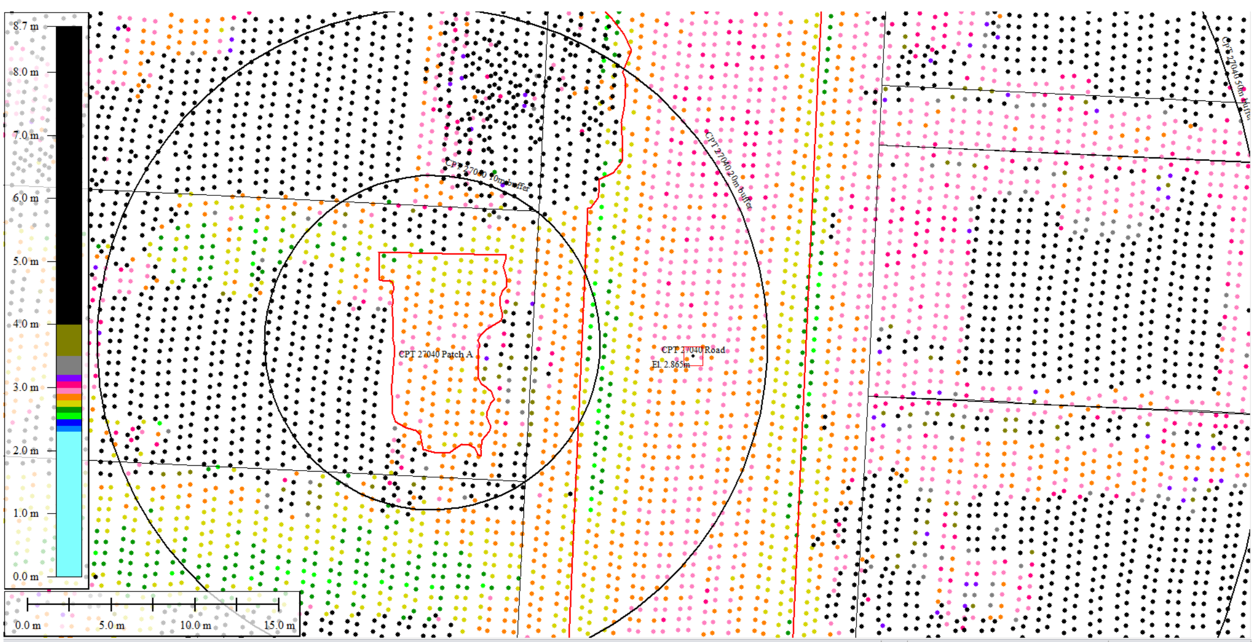

Figure 60: Ground surface elevation averaged over 50-m buffer for Road for Feb 2012 LiDAR survey.

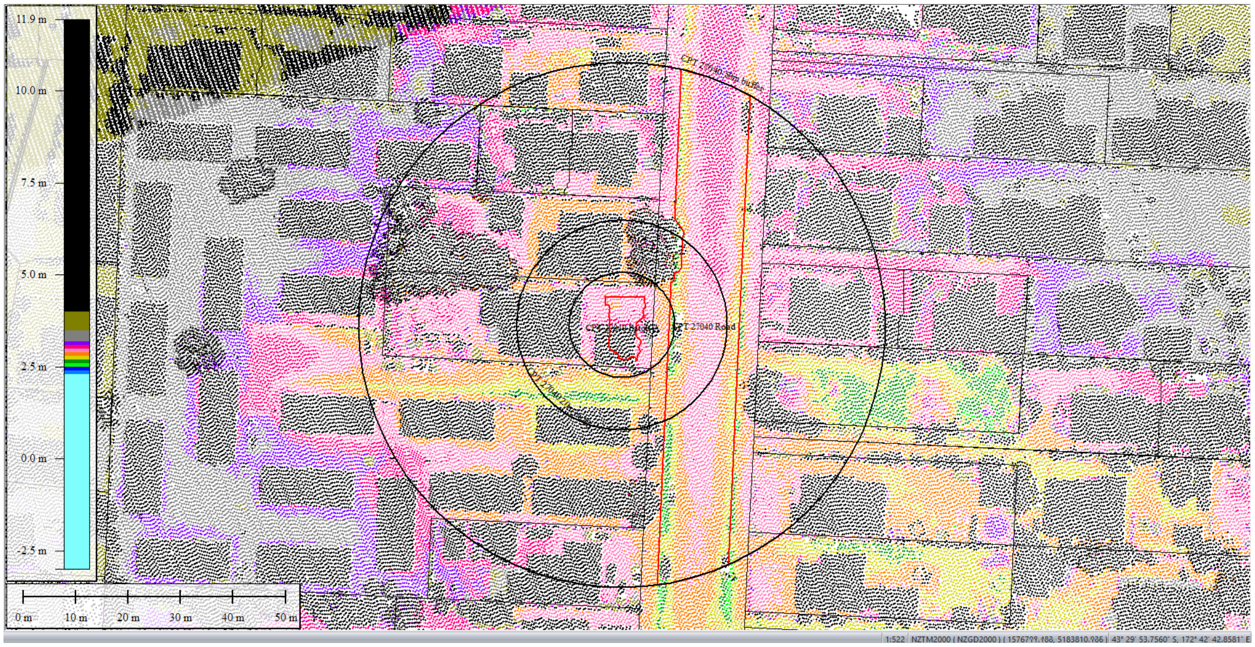

Figure 61: Oct 2015 LiDAR survey.

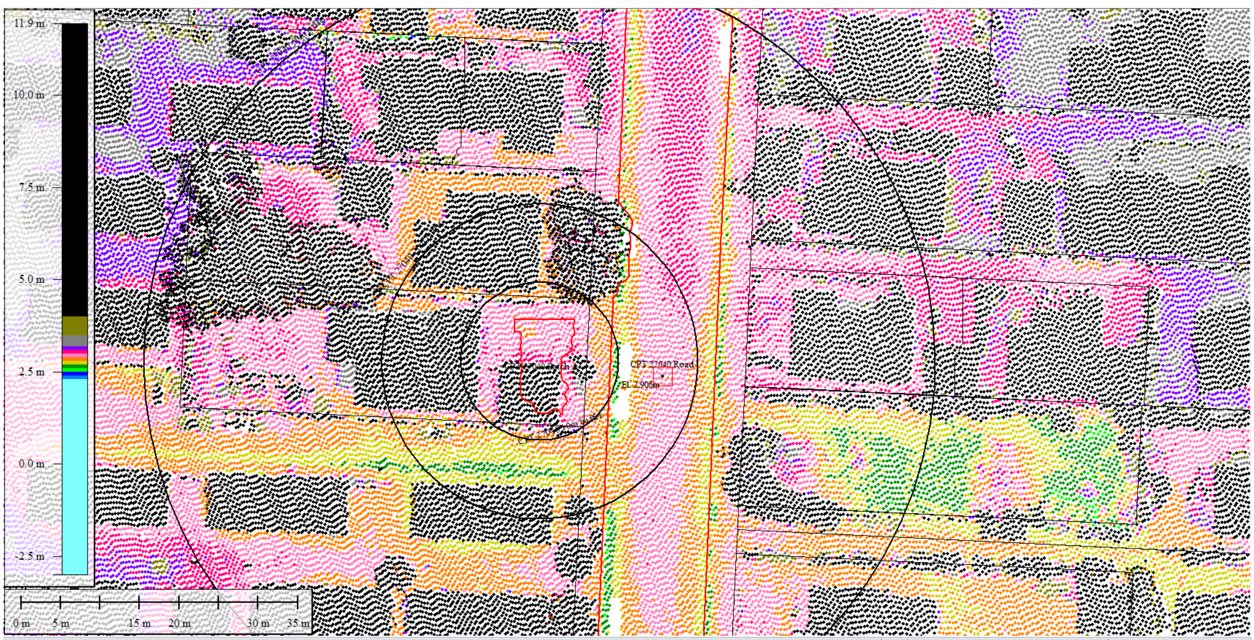

Figure 62: Ground surface elevation averaged over 50-m buffer for Road for Oct 2015 LiDAR survey (el. 2.906m).

Figure 63: Aerial photograph showing the ejecta outline at the site for Feb-11 EQ.

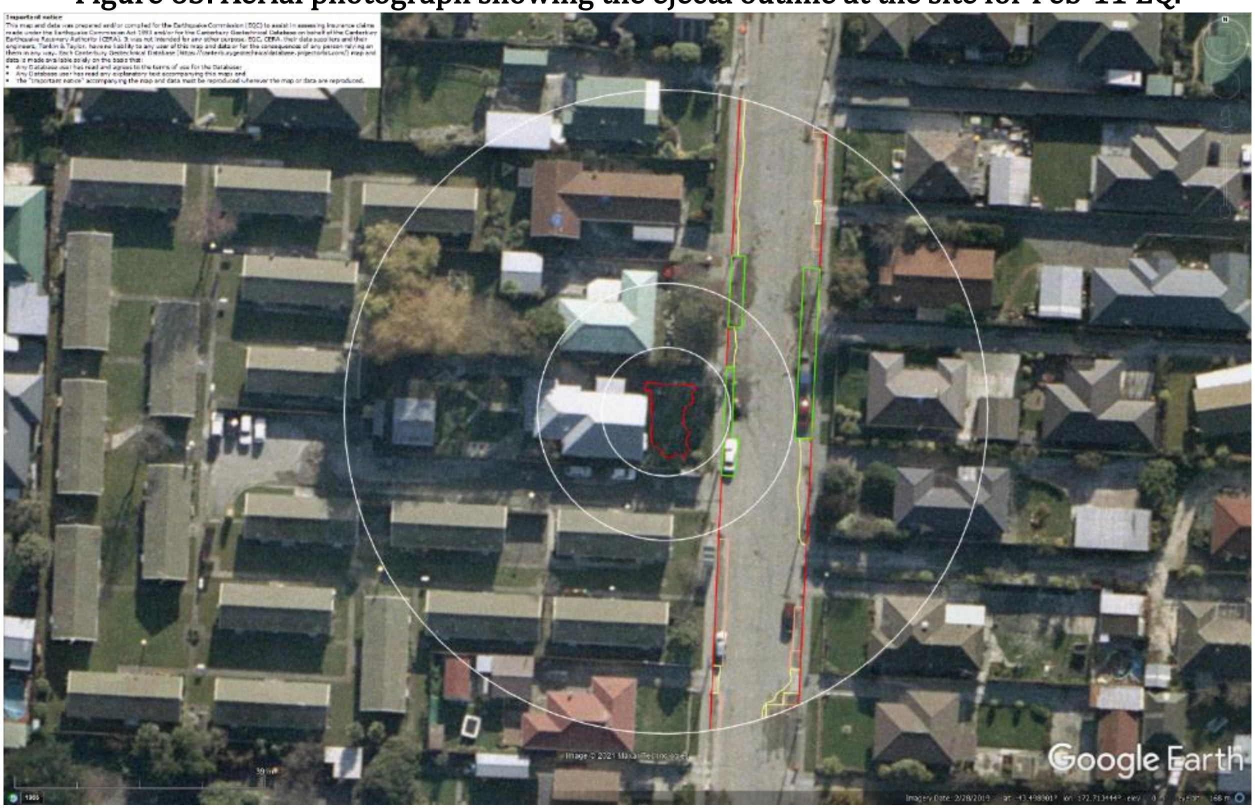

Figure 64: Aerial photograph acquired on 16 Jun 2011 showing the ejecta outline at the site for Jun-11 EQ.

Figure 65: Aerial photograph showing the ejecta outline at the site for Dec-11 EQ.

Contents of this figure cannot be shared as doing so is restricted by a Non-Disclosure Agreement.

Figure 66: LDAT inspection report for the property with Patch A (inspection date: 3 June 2011).

Figure 67: Ground photographs showing ejecta remnants for Patch A (photograph date: 3 June 2011).

Figure 68: Ground photographs showing ejecta remnants at properties within the 50-m buffer (photograph date: 3 June 2011).

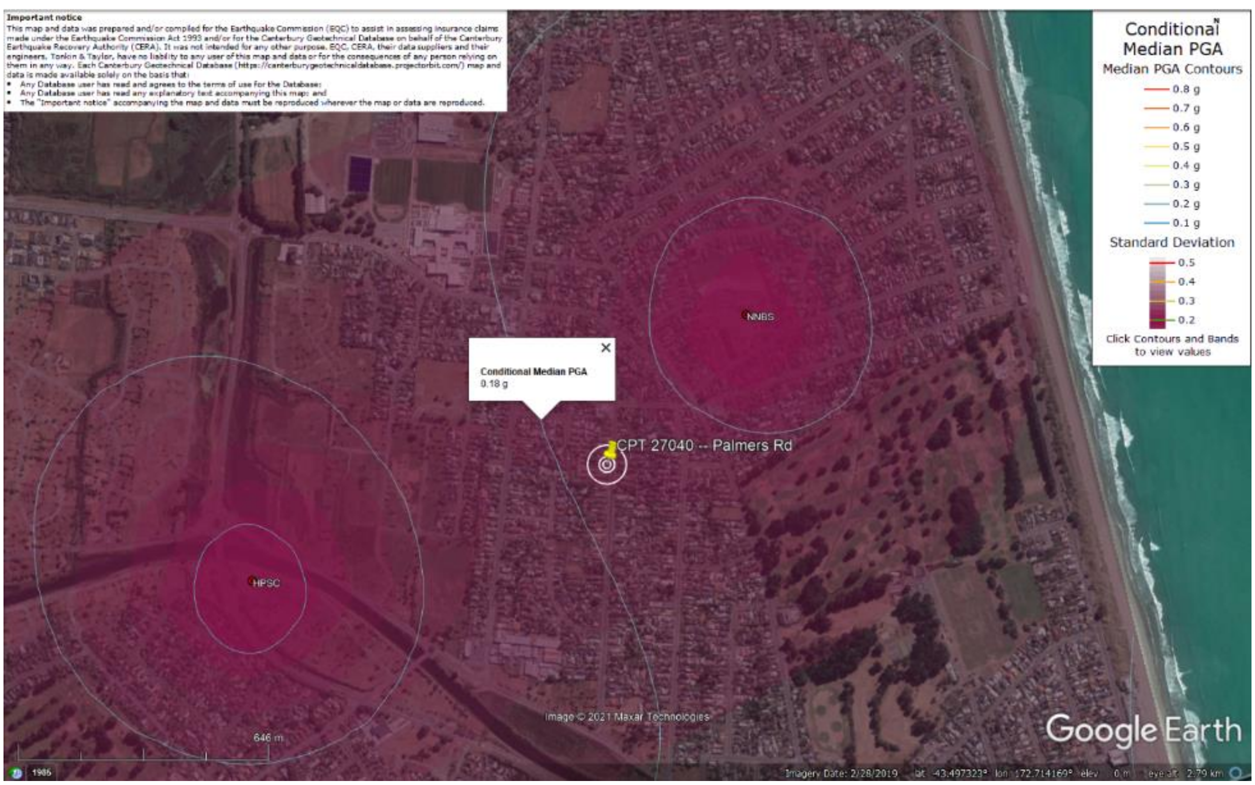

Figure 69: PGA for Sep-10 EQ (st. dev. = 0.225-0.250 ln units).

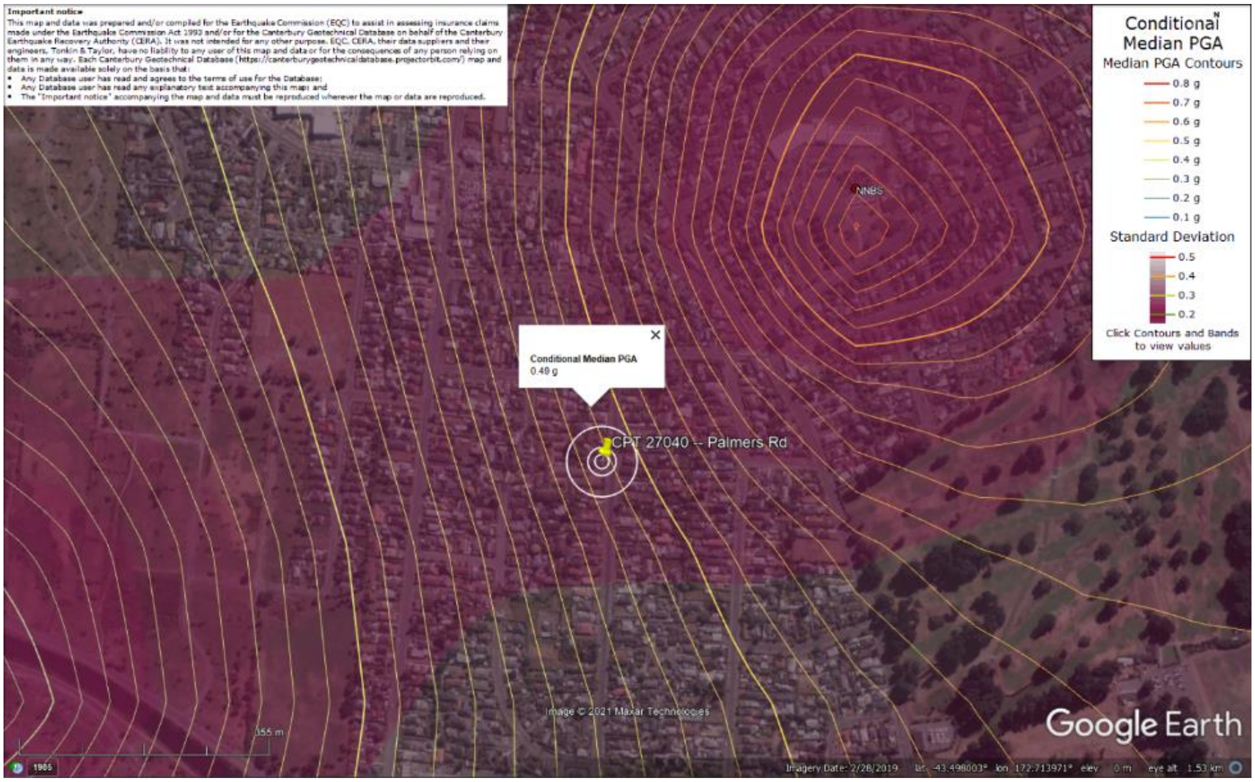

Figure 70: PGA for Feb-11 EQ (st. dev. = 0.250-0.275 ln units).

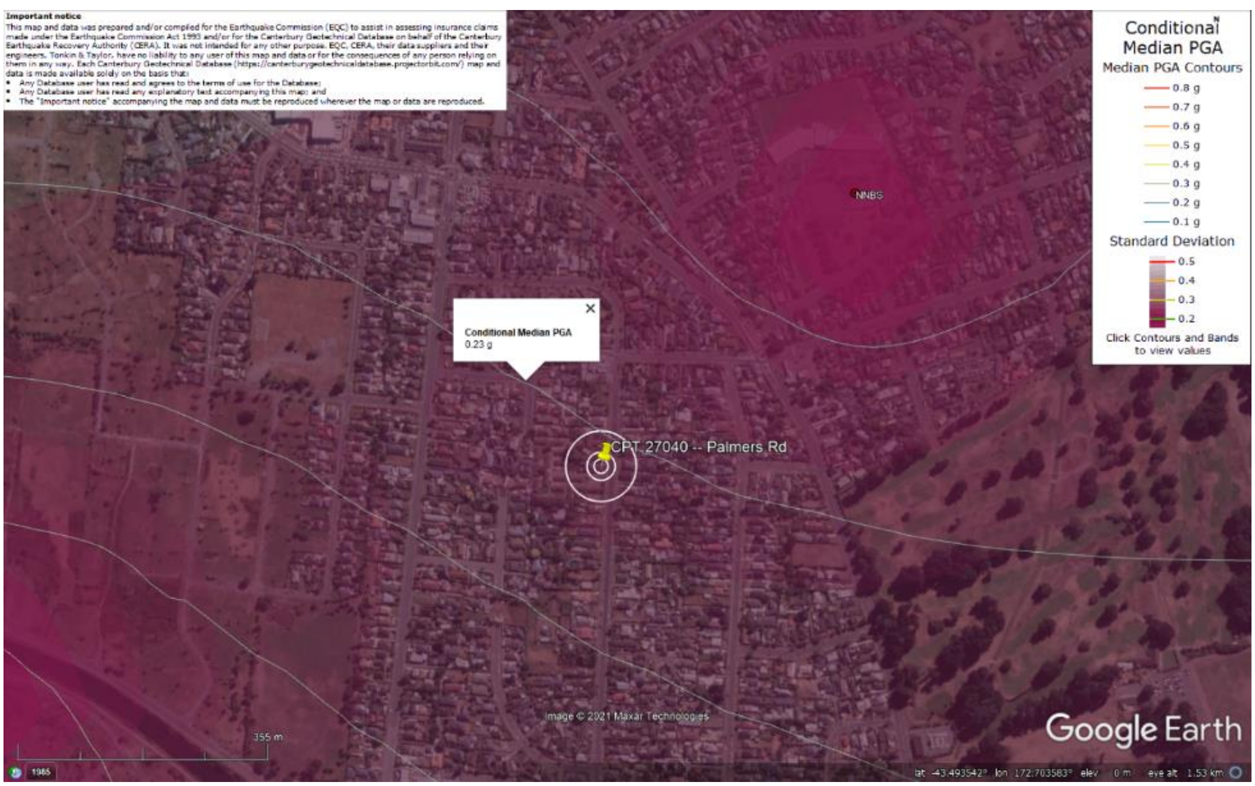

Figure 71: PGA for Jun-11 EQ (st. dev. = 0.250-0.275 ln units).

Figure 72: PGA for Dec-11 EQ (st. dev. = 0.350-0.375 ln units).

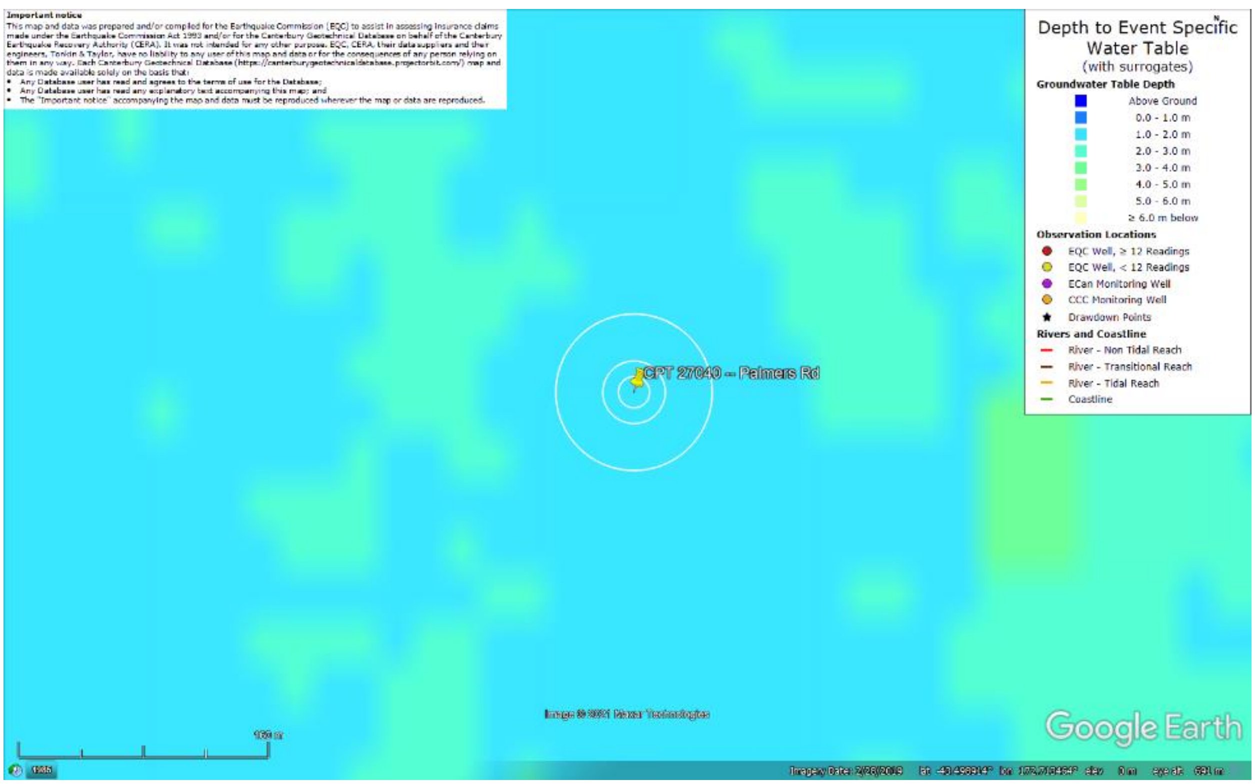

Figure 73: Depth to groundwater table for Sep-10 EQ.

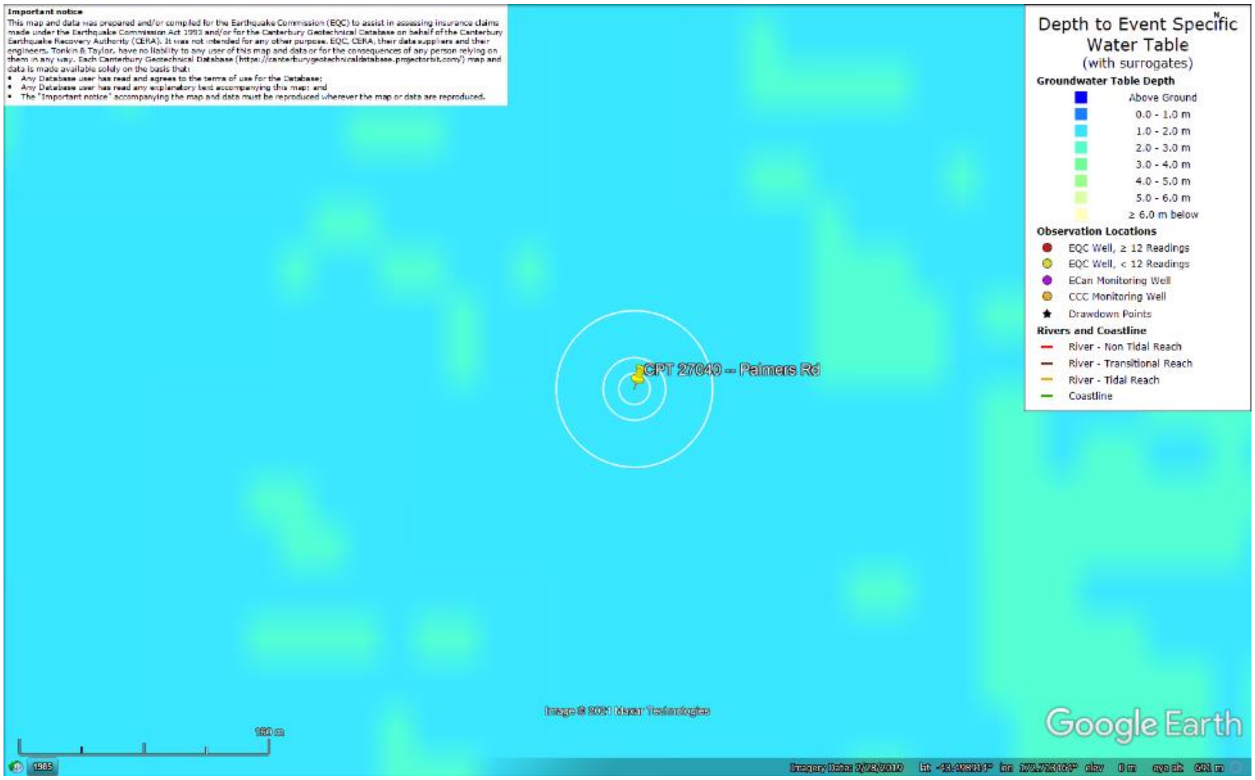

Figure 74: Depth to groundwater table for Feb-11 EQ.

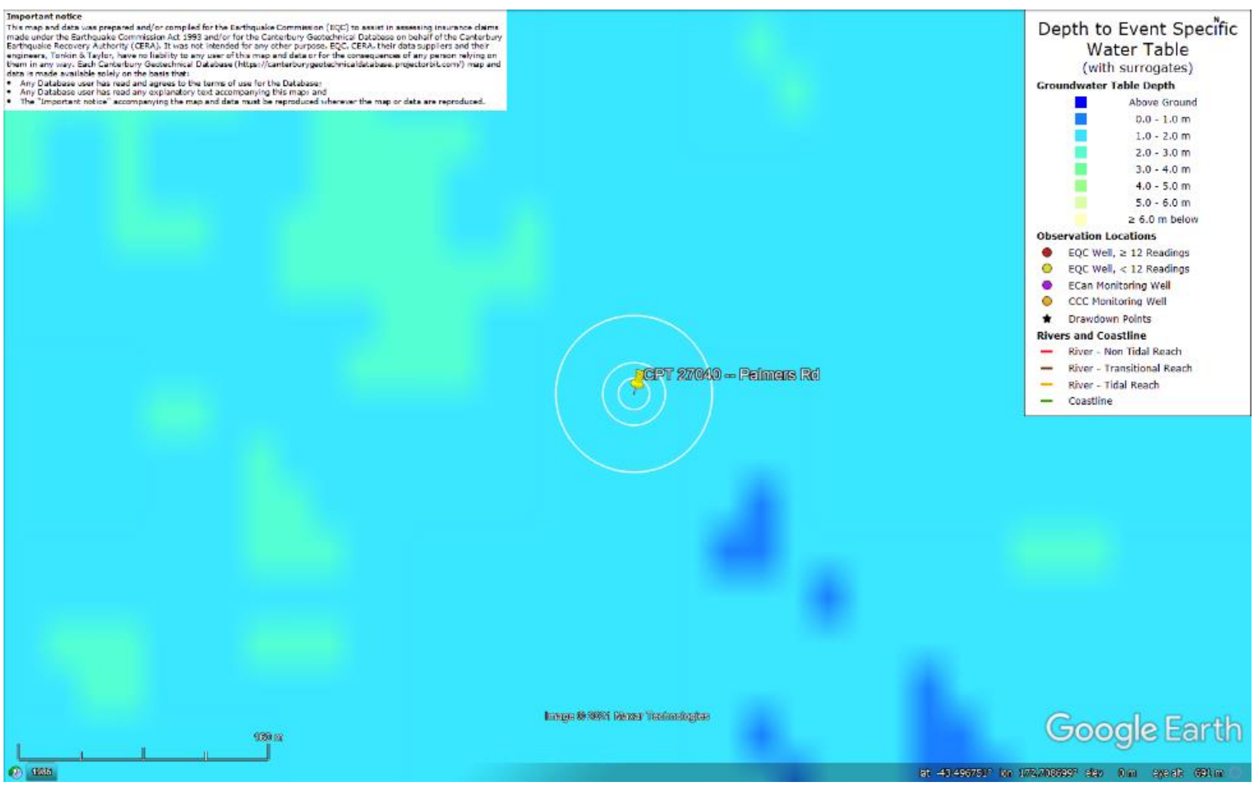

Figure 75: Depth to groundwater table for Jun-11 EQ.

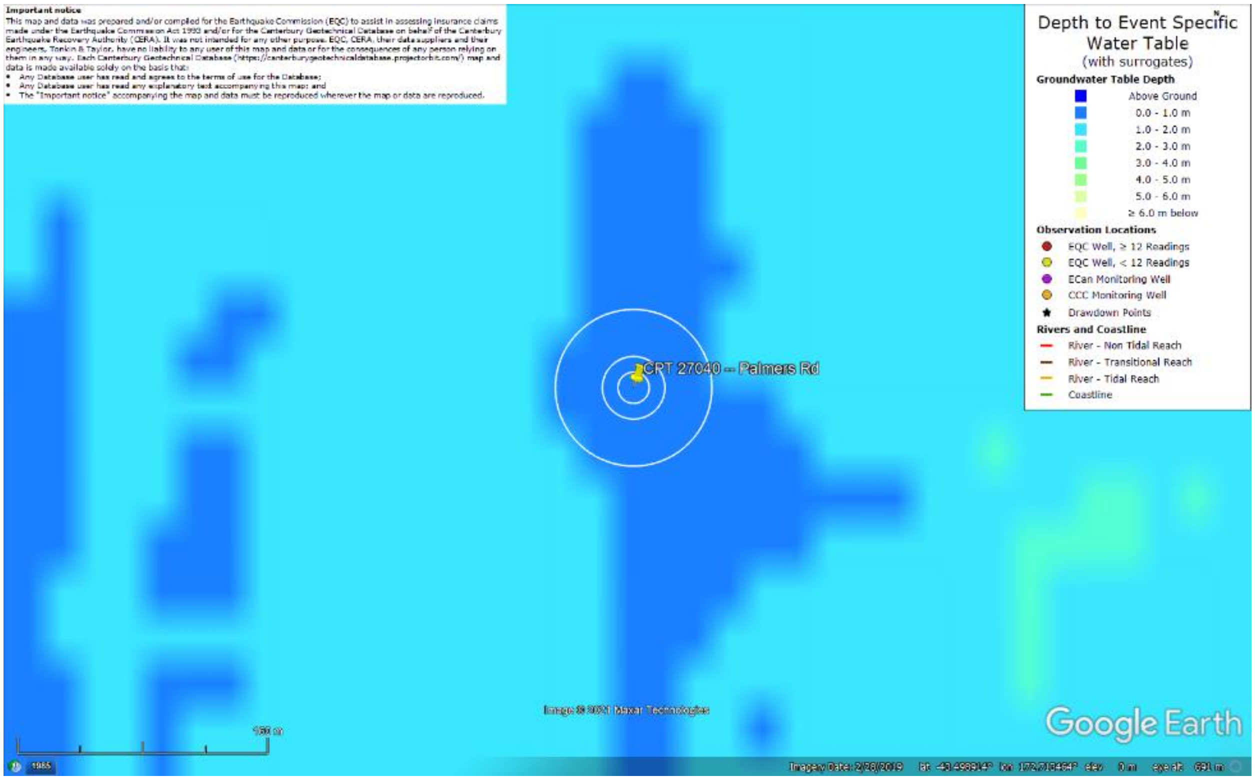

Figure 76: Depth to groundwater table for Dec-11 EQ.

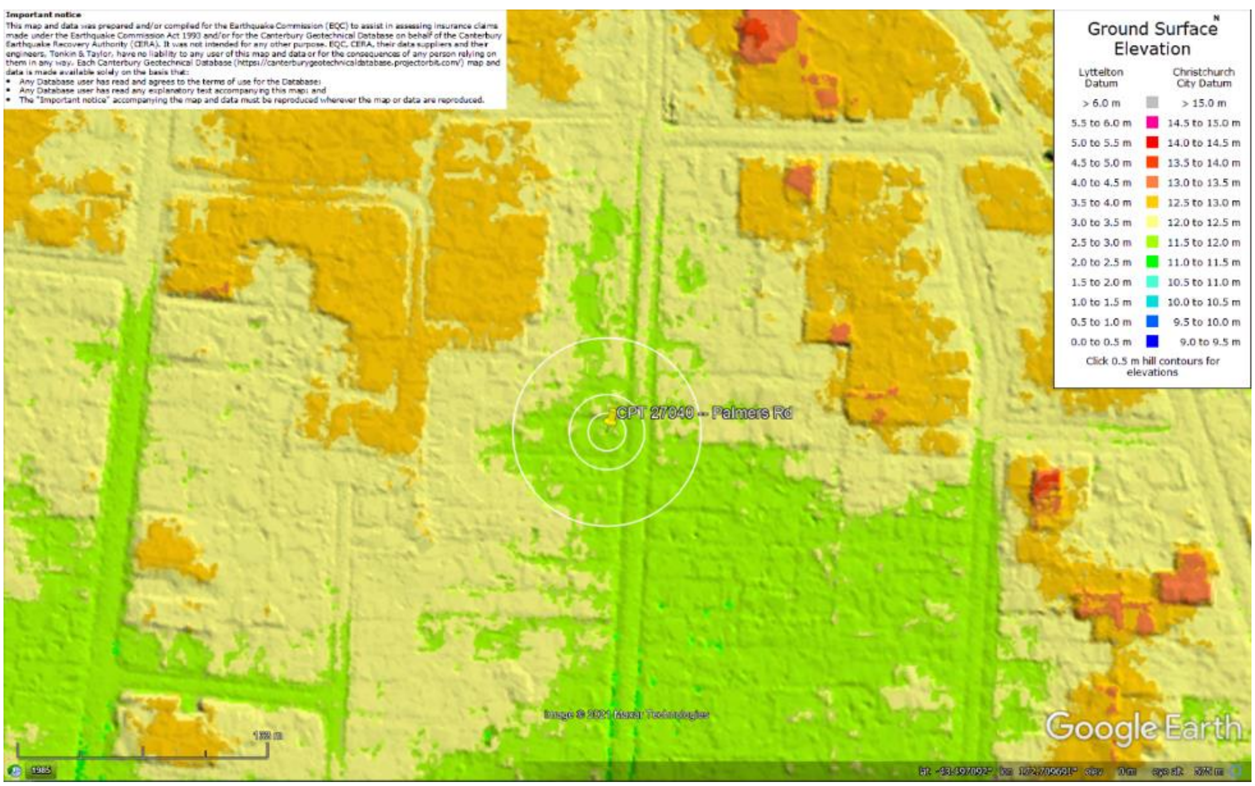

Figure 77: Ground surface elevation according to the Sep-11 LiDAR survey.

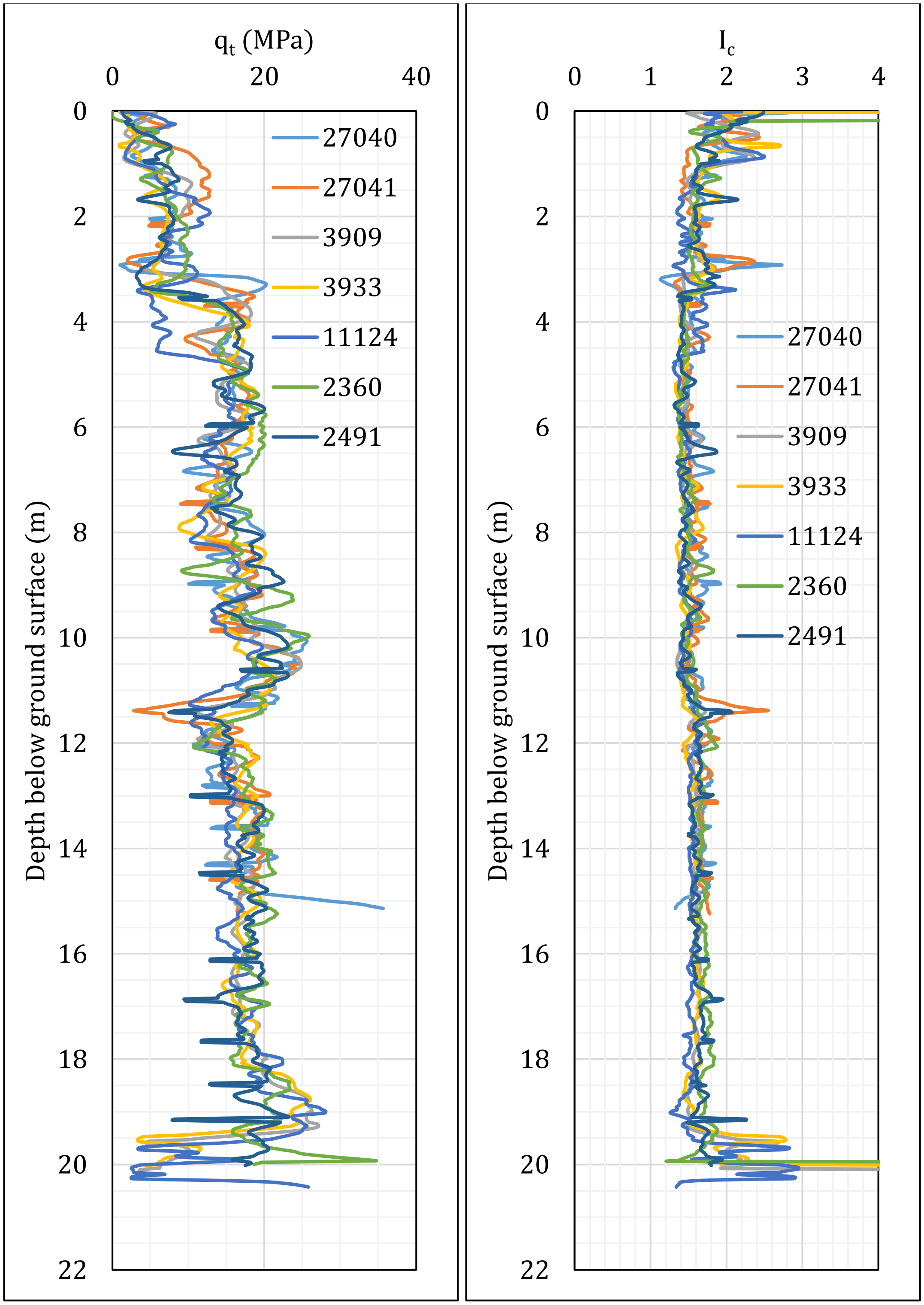

Figure 78: q_t and I_c profiles.

Note 6: The selection of CPTs for the area considered for settlement assessment (Figure 1) is based on the proximity of the CPTs to the considered areas. In accordance with that, the following table shows CPTs that were used for the volumetric settlement analysis in *Cliq v.3.0.3.2*, a CPT soil liquefaction software developed by GeoLogismiki. (The average volumetric settlements were reported in Table 8.)

Table 12: CPT profiles used in volumetric settlement analysis for areas selected for settlement assessment.

CPT ID No.	Patch A	Road (50-m buffer)
27040	✓	✓
27041		
3909		
3933		✓
11124		✓
2360		
2491		✓

Note: CPT 3909 was used to compute the volumetric settlement from 15- to 20-m depth for CPTs 27040 and 27041.

Table 13: CPT-based results.

EQ Event	Parameter	CPT ID 27040	27041	3909	3933	11124	2360	2491	$\Delta_{15m\text{-}20m}$
Sep-10	S_{V1D} (mm)	11	13	6	14	17	2	21	1
	LSN	2	2	1	3	3	1	4	0
	LPI	0	0	0	0	0	0	0	0
	LPI_{ish}	0	0	0	0	0	0	0	--
	$D_{FS<1}$ (m)	undet.	undet.	undet.	3.25	undet.	undet.	undet.	--
Feb-11	S_{V1D} (mm)	46	55	130	140	159	42	120	48
	LSN	11	12	18	28	23	13	24	3
	LPI	4	6	9	13	15	4	11	1
	LPI_{ish}	3	5	7	12	10	2	9	--
	$D_{FS<1}$ (m)	2.06	2.20	1.99	1.41	2.27	1.41	1.42	--
Jun-11	S_{V1D} (mm)	15	18	12	26	33	6	31	2
	LSN	3	4	3	6	6	2	7	0
	LPI	1	1	0	1	1	0	1	0
	LPI_{ish}	1	1	0	0	0	0	1	--
	$D_{FS<1}$ (m)	undet.	undet.	undet.	3.09	3.43	undet.	2.88	--
Dec-11	S_{V1D} (mm)	35	42	80	105	118	33	81	22
	LSN	13	10	19	32	28	14	21	1
	LPI	3	4	5	9	10	3	7	0
	LPI_{ish}	2	3	4	10	9	3	6	--
	$D_{FS<1}$ (m)	0.98	2.20	0.91	0.91	0.91	1.09	1.76	--

Notes: $D_{FS<1}$ = Depth to the first liquefiable layer (FS_L<1) that is at least 200-mm thick, as determined by the Boulanger and Idriss (2016) liquefaction-triggering procedure (P_L=50%, C_{FC}=0.13, and $I_{c,cutoff}$ =2.6), and exported from *Cliq v.3.0.3.2*; undet. = the specified soil layer was not detected; $\Delta_{15m\text{-}20m}$ indicates the amount of S_{V1D}, LSN, and LPI that were added to CPTs 27040 and 27041 due to the shallow penetration depths.

Note 7: Based on the borehole log (BH 2909, Figure 1), the groundwater table is at a depth of 1. 5 m below the ground surface. The soil profile consists of (1) hardfill and topsoil, gravelly organic silt, GM, below asphalt to a depth of 0.35 m and (2) fine to medium sand, SP, of the Christchurch formation to a depth of 20 m.

Note 8: The ejecta-induced free-field settlement provided in Table 11 is an areal average settlement due to ejecta, which is based on the total settlement assessment area, A_T (provided in Table 9 and repeated in Table 14). However, the considered area was not always covered completely with ejecta; thus, it is important to provide the localized ejecta-induced settlement, too. The localized settlement due to ejecta is estimated using photographic evidence only as

$$S_{E,P\_localized} = \frac{V_E}{A_E}$$

where V_E is the total volume of ejecta within A_T and A_E is the total coverage area of ejecta within A_T. Please note that the areal ejecta-induced settlement provided in Table 14 as S_{E,P_areal} is the same as $S_{E,P}$ in Table 11, which was estimated as

$$S_{E,P\_areal} = S_{E,P} = \frac{V_E}{A_T}$$

where V_E is the total volume of ejecta within A_T and A_T is the total settlement assessment area.

Table 14a: Areal and localized ejecta-induced settlement estimates for Patch A (10-, 20-, and 50-m buffers) based on photographic evidence.

Earthquake Event	A_T (m^2)	A_E (m^2)	V_E (m^3)	S_{E,P_areal} (mm)	$S_{E,P\_localized}$ (mm)
Sep-10	62.5	0	0	0	0
Feb-11	62.5	62.5	4.0-7.8	95±30	95±30
Jun-11	62.5	NA	NA	NA	NA
Dec-11	62.5	20.9	0.7-1.2	15±5	45±10

Notes: S_{E,P_areal} = $S_{E,P}$ reported in Table 11 = areal ejecta-induced settlement; $S_{E,P\_localized}$ = localized ejecta-induced settlement; A_T = total settlement assessment area; V_E = total volume of ejecta within A_T; A_E = total area of ejecta within A_T; The estimates of both areal and localized ejecta-induced settlement are rounded to the nearest 5; Final plus/minus values are also rounded to the nearest 5; NA = Not available.

Table 14b: Areal and localized ejecta-induced settlement estimates for Road (50-m buffer) based on photographic evidence.

Earthquake Event	A_T (m^2)	A_E (m^2)	V_E (m^3)	S_{E,P_areal} (mm)	$S_{E,P\_localized}$ (mm)
Sep-10	1291	0	0	0	0
Feb-11	1291	424	5.5-10.9	5±5	20±5
Jun-11	1170	154	1.6-3.1	<5	15±5
Dec-11	1291	94.5	0.4-0.9	<5	5±5

Notes: S_{E,P_areal} = $S_{E,P}$ reported in Table 11 = areal ejecta-induced settlement; $S_{E,P\_localized}$ = localized ejecta-induced settlement; A_T = total settlement assessment area; V_E = total volume of ejecta within A_T; A_E = total area of ejecta within A_T; The estimates of both areal and localized ejecta-induced settlement are rounded to the nearest 5; Final plus/minus values are also rounded to the nearest 5.

<u>**Summary 2:**</u>

- **The best estimate of the <u>localized</u> ejecta-induced free-field ground settlement at the Palmers Rd site for the SEP 2010, FEB 2011, and DEC 2011 earthquake is 0 mm, 95±30 mm, and 45±10 mm, respectively. The localized ejecta-induced settlement for the JUN 2011 earthquake could not be estimated.**
- **The best estimate of the <u>localized</u> ejecta-induced free-field ground settlement of the road at the Palmers Rd site for the SEP 2010, FEB 2011, JUN 2011, and DEC 2011 earthquake is 0 mm, 20±5 mm, 15±5 mm, and 5±5 mm, respectively.**